activity remained unchanged in cells overexpressing Siah-1L or Siah-1 (data not shown). We then investigated the ability of Siah-1L to induce degradation of transiently overexpressed Δβ-catenin (deleted 25–140) or mutant β-catenin (AAAA). As shown in Figure 4c, both Siah-1L and Siah-1 markedly reduced the levels of wild-type β-catenin and β-catenin (AAAA), while the levels of Δβ-catenin (deleted 25–140) remained unchanged. Taken together, these results indicate that β-catenin lacking amino acids 25–140 is resistant to Siah-1-dependent degradation pathways.

Siah-1L sensitizes cancer cells to apoptosis induced by anticancer drugs

To explore the functional significance of p53-inducible Siah-1L in tumor cell survival, we evaluated the ability of Siah-1L to promote apoptosis. MCF7 cells were transiently transfected with plasmids encoding Siah-1L, Siah-1, or Siah-1ΔRING, and cell death was measured 48 h after treatment with DOX. As shown in Figures 5a and b, Siah-1L and Siah-1 enhanced cell death by greater than 50% compared to the control and Siah-1ΔRING-expressing cells. Interestingly, apoptosis-sensitizing effects induced by Siah-1L protein were also observed in p53-null cells (Figures 5c and d). Moreover, similar results were obtained when cell death was induced by cisplatin or UV irradiation in MCF7 and Hep3B cells (data not shown). These data strongly suggest that Siah-1L accelerates cell death induced by anticancer drugs irrespective of the status of endogenous p53 protein.

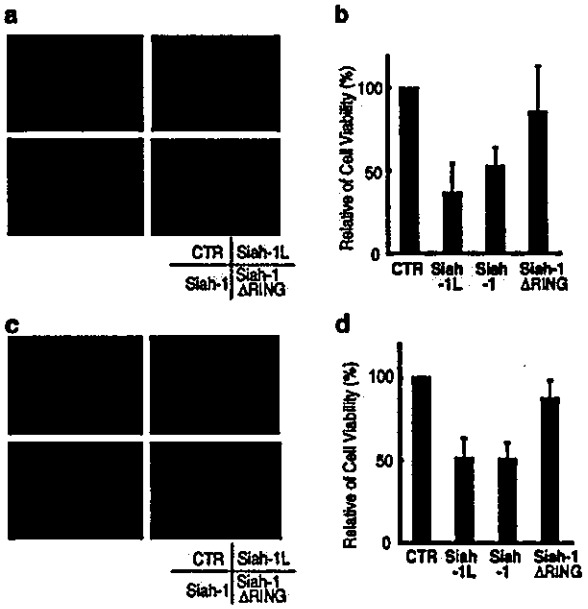

Figure 5 Siah-1L sensitizes cancer cells to apoptotic cell death. MCF7 (**a**, **b**) or Hep3B (**c**, **d**) cells were treated with DOX (1.0 μg/ml) 24 h after transfection of pEGFP-C1 together with empty vector (CTR), pcDNA3-FLAG-Siah-1L (Siah-1L), pcDNA3-FLAG-Siah-1 (Siah-1), or pcDNA3-FLAG-Siah-1ΔRING (Siah-1ΔRING). After 48 h, the GFP-positive viable cells were counted and the relative number of GFP-positive cells was presented

Discussion

It has been suggested that Siah-1 may act as a downstream effector of p53; however, the 5′-flanking region of the Siah-1 gene is known to lack typical TATA or CCAAT boxes and that reporter plasmids containing the promoter region of Siah-1 do not respond to p53 (Maeda *et al*., 2002). Recently, the p53-responsive element has been identified upstream of the alternative in-frame ATG start codon located in the intron 1 of the human Siah-1 gene (Matsuzawa *et al*., unpublished data). In this study, we demonstrated that a novel isoform belonging to the human Siah-1 family, Siah-1L, was identified as a p53-inducible protein.

Dysfunction of the β-catenin degradation pathway results in aberrant accumulation of β-catenin; this is a frequent event in various human cancers, and the aberrant accumulation of β-catenin is reported to trigger oncogenesis and tumor progression (Chung, 2000; Lin *et al*., 2000; Park *et al*., 2001; Ueda M *et al*., 2001; Inagawa *et al*., 2002). However, it has also been shown that aberrant accumulation of β-catenin is not always accompanied by known dysfunction or mutation of the APC, Axin, or β-catenin genes. Recently, Cagatay and Ozturk (2002) demonstrated that aberrant accumulation of β-catenin in tumors is often associated with inactivation of the p53 gene. They also showed that worldwide p53 and β-catenin mutation rates are inversely correlated in HCC (Cagatay and Ozturk, 2002). These data suggest that inactivation of p53 may be an important cause of aberrant accumulation of β-catenin in cancer cells. However, the molecular mechanism by which p53 regulates β-catenin activity has been unclear. In this study, we have demonstrated that the expression level of Siah-1L is regulated in a p53-dependent manner in cells with wild-type p53. In contrast, in p53-null cells, no induction of Siah-1L was observed after p53-activating stimuli, resulting in the sustained accumulation of β-catenin protein. Moreover, using specific siRNA for Siah-1L, p53-induced degradation of β-catenin was almost rescued. These results suggest that lack of Siah-1L, but not Siah-1, expression in response to p53 may contribute to the aberrant accumulation of β-catenin in cells harboring p53 mutations. It is important to note that overexpression of Siah-1L in p53-null cells led to the degradation of the accumulated endogenous β-catenin protein, indicating that aberrant accumulation of β-catenin can be reversed by exogenously expressed Siah-1-family proteins in cancer cells regardless of p53 status.

β-Catenin with mutations in the GSK3β phosphorylation sites has been observed in various human cancers. For example, mis-sense mutations at codons 32, 34, 37, or 41, which affect the GSK3β phosphorylation sites of β-catenin, were also common in HCC (Wong *et al*., 2001; Cagatay and Ozturk, 2002). Siah-family proteins trigger the degradation of β-catenin protein regardless of the GSK3β-mediated phosphorylation of β-catenin. Thus, our data indicate that activation of Siah-1L-dependent β-catenin degradation, including the overexpression of exogenous Siah-1L proteins, may

represent a powerful approach to the treatment of cancers with aberrant accumulation of β-catenin and dysregulated Wnt/β-catenin signalling. On the other hand, constitutive activation of β-catenin caused by deletions in exons 3 and 4 was found in some human cancers (de La Coste *et al.*, 1998). Therefore, we must draw attention to the finding that overexpression of Siah-1-family protein had little effect on the degradation of this mutant β-catenin found in HepG2 cells. Further analysis of the Siah-1/SIP/Ebi pathway for β-catenin degradation is necessary to find a strategy to counteract the various types of mutant β-catenin protein.

We have concluded that p53-dependent expression of Siah-1L but not Siah-1 plays an important role in the regulation of β-catenin activity in human tumor cells. These results suggest new strategies for restoring tumor suppressive pathways caused by p53 inactivation.

Materials and methods

Plasmids

The cDNA encoding human Siah-1L was generated by RT–PCR from the mRNA of MCF7 cells treated with DOX using SuperScript II (Invitrogen, San Diego, CA, USA), followed by PCR amplification using the KOD-Plus-DNA polymerase system (TOYOBO, Osaka, Japan) and the following oligonucleotide primers: 5′-GACGAATTCATGGTTATAATTAT TTTTCT-3′ (sense) and 5′-GACCTCGAGTCAACACATGG AAATAGTTAC-3′ (antisense). The resulting PCR fragments were inserted into the *Eco*RI–*Xho*I sites of pcDNA3-FLAG (Matsuzawa and Reed, 2001). pcDNA3-FLAG-Siah-1 and pcDNA3-FLAG-Siah-1ΔRING plasmids were constructed by inserting the *Eco*RI–*Xho*I fragments from the pcDNA3-Myc-Siah-1 and pcDNA3-Myc-Siah-1ΔRING plasmids into the pcDNA3-FLAG vector (Matsuzawa and Reed, 2001). pRC-CMV-p53 (wild type) and pRC-CMV-p53 (179Mut) were described previously (Unger *et al.*, 1992). The expression plasmid encoding β-catenin, pcDNA3-Myc-β-catenin, was described previously (Ueda Y *et al.*, 2001). The cDNAs encoding various β-catenin mutants were generated by two-step PCR amplification. Briefly, to construct β-catenin (AAAA), which has alanine substitutions at the putative GSK3β phosphorylation sites (serine or threonine amino-acid residues at positions 33, 37, 41, and 45), a DNA fragment encoding amino acids 1–37, a fragment encoding amino acids 33–50, and a fragment encoding amino acids 44–781 were separately PCR amplified with the following primer sets: BCAT-fullS, 5′-GGATCCGTATGGCTACTCAAGCTGAT TT-3′, BCAT-37AS, 5′-AGCATGGATTCCAGCGTCCAGG TAAGAC-3′; BCAT-33S, 5′-GCTGGAATCCATGCTGGT GCCACTGCCACTGCCACAGCT-3′, BCAT-50AS, 5′-GCC TTTACCACTCAGAGCAGGAGCTGTGGCAGTGGC-3′; BCAT-44S, 5′-CCTGCTCTGAGTGGTAAAGGC-3′, BCAT-fullAS, 5′-TCTAGATTACAGGTCAGTATCAAACC-3′. The resulting PCR fragments were mixed and subjected to a second PCR reaction to obtain full-length β-catenin (AAAA) containing *Bam*HI and *Xba*I sites. To construct Δβ-catenin (deleted 25–140), which lacks amino acids 25–140, DNA fragments encoding the amino- and carboxyl-terminal regions were separately PCR amplified with primer sets BCAT-fullS and BCAT-25AS (5′-GTGACTAACAGCCGCTTTTC-3′) and BCAT-120S (5′-GTGTTGTTTTATGCCATTAC-3′) and BCAT-fullAS, respectively. The two PCR products were mixed and subjected to a second PCR reaction to obtain full-length Δβ-catenin (deleted 25–140) containing *Bam*HI and *Xba*I sites. These products were subcloned into the *Bam*HI and *Xba*I sites of the pcDNA3-Myc plasmid (Matsuzawa and Reed, 2001). The reporter plasmids pTcf7wt-Luc and pTcf7mut-Luc have been described previously (Ueda Y *et al.*, 2001). All constructs were confirmed by DNA sequencing.

Cell culture and transfection

Human breast cancer MCF7 cells, hepatoma Hep3B cells, hepatoblastoma HepG2 cells, and human embryonic kidney HEK293T cells were maintained in Dulbecco's modified Eagle's medium (Nissui, Tokyo, Japan) supplemented with 10% FBS, and L-glutamine at 37°C in an atmosphere containing 5% CO_2. In some cases, cells were exposed to DOX, 10 J/m² UV irradiation, or 5 μM MG132 (Peptide Institute, Osaka, Japan). For transfection of plasmids into the cells, we used the FuGENE6 transfection reagent (Roche, Indianapolis, IN, USA) according to the manufacturer's protocol. The amount of plasmid DNA in each transfection was kept constant by the addition of an appropriate amount of empty expression vector.

siRNA transfections

We designed the following siRNA duplexes within the open reading frame of Siah-1L to knock down Siah-1L. The siRNA duplexes were synthesized and purified by Qiagen Inc. (Cambridge, MA, USA). Siah-1L target sequence was as follows: siSiah-1L, 5′-AACTCCTGCCTCCTTATGTATTT-3′. The nonsilencing siRNA (control siRNA) was as follows: siCTR, 5′-AAGAGCCGTCAGACTGCTACA-3′. For transient transfections, cells were seeded at a density of 40–50% in 60 mm diameter plates. The following day, transfections of siRNAs were performed by using Lipofectamine 2000 reagent (Invitrogen), according to the manufacturer's recommended protocol.

Preparation of RNA and RT–PCR

Total RNA was extracted using Sepasol-RNA I Super (Nacalai Tesque, Kyoto, Japan) according to the manufacturer's protocol. RT–PCR was performed using the One Step RNA PCR Kit (Takara, Tokyo, Japan) according to the manufacturer's protocol. The PCR primers for amplification of Siah-1L, Siah-1, and GAPDH were as follows: Siah-1L-3S, 5′-GGTTATAATTATTTTTCTCCTGCCTCC-3′ and Siah-1&1L-512AS, 5′-AGTCAACAGCACCAGGAAGA-3′; Siah-1-minus18S, 5′-CGCTCTCCGCCCACAGAAAT-3′ and Siah-1&1L-512AS; GAPDH-1S, 5′-ATGGGGAAGGTGAAGGT CGG-3′ and GAPDH-837AS, 5′-TGGAGGGATCTCGCTC CTGG-3′.

Western blot analyses

Protein samples were diluted in 2× sodium dodecyl sulfate (SDS) sample buffer (62.5 mM Tris-HCl, pH 6.8, 2% SDS, 5% β-mercaptoethanol, 10% glycerol, and 0.002% bromophenol blue). Samples were separated by 10% SDS–polyacrylamide gel electrophoresis (PAGE). After electrotransfer, polyvinylidene difluoride membranes were probed with primary antibodies and secondary antibodies conjugated to HRP. The antibodies used in these experiments were anti-β-catenin (Transduction Laboratories, Lexington, KY, USA), anti-p53 (Ab-6) (Calbiochem), anti-c-Myc (9E10) (Santa Cruz Biotechnology Inc., Santa Cruz, CA, USA), anti-FLAG M2 (Sigma, St Louis, MO, USA), anti-α-actin (Sigma), and goat

polyclonal anti-Siah-1 (Abcam, Cambridge, UK). Immunocomplexes were detected by the enhanced chemiluminescence assay (NEN Life Science, Boston, MA, USA).

Reporter assays

To determine Tcf/LEF activity, subconfluent cells were transfected with a reporter construct (pTCF7wt-Luc or pTCF7mut-Luc) and various expression plasmids. A thymidine kinase (TK)-expressing vector (pRL-TK; Promega, Madison, WI, USA) was included as an internal control for transfection efficiency. After 30 h, the cells were lysed and both the luciferase and TK activities were determined using a luciferase assay kit (Promega). Tcf/LEF reporter activities were normalized relative to TK activities and were presented as mean$\pm$s.d. from at least three independent experiments.

Evaluation of cell death

MCF7 and Hep3B cells were grown on plastic dishes as monolayers. Cells were transfected with pEGFP-C1 (BD Biosciences Clontech) and various expression plasmids encoding Siah-1L, Siah-1, or Siah-1ΔRING or empty vector (CTR) for 12 h, followed by treatment with DOX. After 48 h, the GFP-positive cells were counted using a Zeiss AxioVert200 (Zeiss, Hallbergmoos, Germany). The histogram is presented as the average$\pm$s.d. of three independent experiments, and the relative survival rate was determined by normalizing to the number of GFP-positive cells transfected with empty vector.

Abbreviations

APC, adenomatous polyposis coli; GSK3β, glycogen synthase kinase 3β; SIP, Siah interacting protein; HCC, hepatocellular carcinoma; RT–PCR, reverse-transcriptase polymerase chain reaction; DOX, doxorubicin; siRNA, short interfering RNA; Tcf, T-cell factors; LEF, lymphocyte enhancer-binding factor; SDS–PAGE, sodium dodecyl sulfate–polyacrylamide gel electrophoresis; TK, thymidine kinase.

Acknowledgements

This work was supported by grants-in-aid for cancer research and for the second-term comprehensive 10-year strategy for cancer control and the Ministry of Health, Labor, and Welfare, through grants-in-aid for scientific research from the Ministry of Education, Culture, Sports, Science, and Technology, grants-in-aid of Research for the Future from the Japanese Society for the Promotion of Science, and by the Program for Promotion of Fundamental Studies in Health Science of the Organization for Pharmaceutical Safety and Research (OPSR) of Japan.

References

Cagatay T and Ozturk M. (2002). *Oncogene*, **21**, 7971–7980.
Chung DC. (2000). *Gastroenterology*, **119**, 854–865.
de La Coste A, Romagnolo B, Billuart P, Renard CA, Buendia MA, Soubrane O, Fabre M, Chelly J, Beldjord C, Kahn A and Perret C. (1998). *Proc. Natl. Acad. Sci. USA*, **95**, 8847–8851.
Della NG, Senior PV and Bowtell DD. (1993). *Development*, **117**, 1333–1343.
Devereux TR, Stern MC, Flake GP, Yu MC, Zhang ZQ, London SJ and Taylor JA. (2001). *Mol. Carcinogen.*, **31**, 68–73.
Fiucci G, Beaucourt S, Duflaut D, Lespagnol A, Stumptner-Cuvelette P, Geant A, Buchwalter G, Tuynder M, Susini L, Lassalle JM, Wasylyk C, Wasylyk B, Oren M, Amson R and Telerman A. (2004). *Proc. Natl. Acad. Sci. USA*, **101**, 3510–3515.
Hart MJ, de los Santos R, Albert IN, Rubinfeld B and Polakis P. (1998). *Curr. Biol.*, **8**, 573–581.
Hu G, Chung YL, Glover T, Valentine V, Look AT and Fearon ER. (1997a). *Genomics*, **46**, 103–111.
Hu G, Zhang S, Vidal M, Baer JL, Xu T and Fearon ER. (1997b). *Genes Dev.*, **11**, 2701–2714.
Inagawa S, Itabashi M, Adachi S, Kawamoto T, Hori M, Shimazaki J, Yoshimi F and Fukao K. (2002). *Clin. Cancer Res.*, **8**, 450–456.
Lee TK, Lau TC and Ng IO. (2002). *Cancer Chemother. Pharmacol.*, **49**, 78–86.
Lin SY, Xia W, Wang JC, Kwong KY, Spohn B, Wen Y, Pestell RG and Hung MC. (2000). *Proc. Natl. Acad. Sci. USA*, **97**, 4262–4266.
Liu J, Stevens J, Rote CA, Yost HJ, Hu Y, Neufeld KL, White RL and Matsunami N. (2001). *Mol. Cell*, **7**, 927–936.
Maeda A, Yoshida T, Kusuzaki K and Sakai T. (2002). *FEBS Lett.*, **512**, 223–226.
Matsuzawa S and Reed JC. (2001). *Mol. Cell*, **7**, 915–926.
Matsuzawa S, Takayama S, Froesch BA, Zapata JM and Reed JC. (1998). *EMBO J.*, **17**, 2736–2747.
Omer CA, Miller PJ, Diehl RE and Kral AM. (1999). *Biochem. Biophys. Res. Commun.*, **256**, 584–590.
Park WS, Oh RR, Park JY, Kim PJ, Shin MS, Lee JH, Kim HS, Lee SH, Kim SY, Park YG, An WG, Jang JJ, Yoo NJ and Lee JY. (2001). *J. Pathol.*, **193**, 483–490.
Peifer M and Polakis P. (2000). *Science*, **287**, 1606–1609.
Provost E and Rimm DL. (1999). *Curr. Opin. Cell Biol.*, **11**, 567–572.
Relaix F, Wei X-J, Li W, Pan J, Lin Y, Bowtell DD, Sassoon DA and Wu X. (2000). *Proc. Natl. Acad. Sci. USA*, **97**, 2105–2110.
Roperch JP, Lethrone F, Prieur S, Piouffre L, Israeli D, Tuynder M, Nemani M, Pasturaud P, Gendron MC, Dausset J, Oren M, Amson RB and Telerman A. (1999). *Proc. Natl. Acad. Sci. USA*, **96**, 8070–8073.
Satoh S, Daigo Y, Furukawa Y, Kato T, Miwa N, Nishiwaki T, Kawasoe T, Ishiguro H, Fujita M, Tokino T, Sasaki Y, Imaoka S, Murata M, Shimano T, Yamaoka Y and Nakamura Y. (2000). *Nat. Genet.*, **24**, 245–250.
Ueda M, Gemmill RM, West J, Winn R, Sugita M, Tanaka N, Ueki M and Drabkin HA. (2001). *Br. J. Cancer*, **85**, 64–68.
Ueda Y, Hijikata M, Takagi S, Takada R, Takada S, Chiba T and Shimotohno K. (2001). *Biochem. Biophys. Res. Commun.*, **283**, 327–333.
Unger T, Nau MM, Segal S and Minna JD. (1992). *EMBO J.*, **11**, 1383–1390.
Wong CM, Fan ST and Ng IO. (2001). *Cancer*, **92**, 136–145.
Yost C, Torres M, Miller JR, Huang E, Kimelman D and Moon RT. (1996). *Genes Dev.*, **10**, 1443–1454.

THE JOURNAL OF BIOLOGICAL CHEMISTRY
Vol. 280, No. 13, Issue of April 1, pp. 12430–12437, 2005
Printed in U.S.A.

Centrosomal P4.1-associated Protein Is a New Member of Transcriptional Coactivators for Nuclear Factor-κB*

Received for publication, September 10, 2004, and in revised form, January 13, 2005
Published, JBC Papers in Press, January 31, 2005, DOI 10.1074/jbc.M410420200

Michiyo Koyanagi‡, Makoto Hijikata, Koichi Watashi, Osamu Masui, and Kunitada Shimotohno§

From the Department of Viral Oncology, Institute for Virus Research, Kyoto University, Sakyo-ku, Kyoto 606-8507, Japan

Nuclear factor-κB (NF-κB) is a transcription factor important for various cellular events such as inflammation, immune response, proliferation, and apoptosis. In this study, we performed a yeast two-hybrid screening using the N-terminal domain of the p65 subunit (RelA) of NF-κB as bait and isolated centrosomal P4.1-associated protein (CPAP) as a candidate for a RelA-associating partner. Glutathione *S*-transferase pull-down assays and co-immunoprecipitation experiments followed by Western blotting also showed association of CPAP with RelA. When overexpressed, CPAP enhanced NF-κB-dependent transcription induced by tumor necrosis factor-α (TNFα). Reduction of the protein level of endogenous CPAP by RNA interference resulted in decreased activation of NF-κB by TNFα. After treatment with TNFα, a portion of CPAP was observed to accumulate in the nucleus, although CPAP was found primarily in the cytoplasm without any stimulation. Moreover, CPAP was observed in a complex recruited to the transcriptional promoter region containing the NF-κB-binding motif. One hybrid assay showed that CPAP has the potential to activate gene expression when tethered to the transcriptional promoter. These data suggest that CPAP functions as a coactivator of NF-κB-mediated transcription. Since a physiological interaction between CPAP and the coactivator p300/CREB-binding protein was also observed and synergistic activation of NF-κB-mediated transcription was achieved by these proteins, CPAP-dependent transcriptional activation is likely to include p300/CREB-binding protein.

Nuclear factor-κB (NF-κB)[1] is a Rel transcription factor that regulates the expression of a wide variety of genes involved in cellular events such as inflammation, immune response, proliferation, and apoptosis (1–3). Rel family members form hetero- and homodimers that possess distinct specificities and functions. In mammals, five Rel family members have been identified: c-Rel, RelA/p65, RelB, NF-κB1 (p50/p105), and NF-κB2 (p52/p100). In the canonical NF-κB signaling pathway, the prototypical NF-κB complex composed of p50 and RelA subunits is sequestered in the cytoplasm through its assembly with a family of NF-κB inhibitors (IκB) at steady state. When cells are stimulated by signals such as tumor necrosis factor-α (TNFα) and interleukin-1, IκB is phosphorylated by the IκB kinase complex, marking it for ubiquitination and subsequent degradation. The liberated NF-κB heterodimer rapidly translocates into the nucleus and activates target genes by binding directly to κB regulatory elements present in the target loci.

Although these cytoplasmic signaling events are understood in detail, the subsequent nuclear events that regulate the strength and duration of NF-κB-mediated transcriptional activation remain poorly defined (4). RelA contains a transactivation domain (TAD) in its C-terminal region that is known to be responsible for transcriptional activation. TAD has so far been reported to interact with various transacting and basal transcription factors that recruit RNA polymerase II, including TATA-binding protein, transcription factor IIB, $TAF_{II}105$ (TATA-binding protein-associated factor II105), and TLS (translocated in liposarcoma) (5–8). In addition, general coactivators such as cAMP response element-binding protein (CREB)-binding protein (p300/CBP) (9, 10), p300/CBP-associated factor, and ACTR (coactivator for nuclear hormone receptors) are recruited to the NF-κB transcriptional complex and enhance NF-κB-mediated transcriptional activation (11, 12).

The N-terminal domain of RelA is also known to play important roles in the regulation of NF-κB-mediated transcriptional activation. For example, stimulus-coupled phosphorylation of RelA is known to change its transcriptional activity (4, 10, 13–16), and two of the four serine phosphoacceptor sites present in RelA are in the N-terminal domain. In addition, association with p300/CBP has been reported to occur not only via TAD, but also through the N-terminal domain of RelA. RelA phosphorylation at Ser^{276} by the catalytic subunit of cAMP-dependent protein kinase (14) or mitogen- and stress-activated protein kinase-1 (15) or at Ser^{311} by protein kinase Cζ (16) was shown to enhance the binding of p300/CBP to RelA. Moreover, p300/CBP has also been reported to acetylate RelA at three sites in the N-terminal domain: Lys^{218}, Lys^{221}, and Lys^{310}. Acetylation is thought to regulate the transcriptional activity of RelA by increasing its DNA-binding affinity for the κB enhancer or by preventing its association with IκBα (4, 17–20). Finally, BRCA1 also associates with the N-terminal domain of

* This work was supported in part by grants-in-aid for cancer research and for the second-term comprehensive 10-year strategy for cancer control from the Ministry of Health, Labor, and Welfare of Japan, by grants-in-aid for scientific research from the Ministry of Education, Culture, Sports, Science, and Technology of Japan, by grants-in-aid for research for the future from the Japanese Society for the Promotion of Science, and by the Program for Promotion of Fundamental Studies in Health Science of the Organization for Pharmaceutical Safety and Research of Japan. The costs of publication of this article were defrayed in part by the payment of page charges. This article must therefore be hereby marked "*advertisement*" in accordance with 18 U.S.C. Section 1734 solely to indicate this fact.

‡ Supported by the 21st Century Center of Excellence Program of the Ministry of Education, Culture, Sports, Science, and Technology of Japan to the Graduate School of Biostudies and the Institute for Virus Research, Kyoto University.

§ To whom correspondence should be addressed. Tel.: 81-75-751-4000; Fax: 81-75-751-3998; E-mail: kshimoto@virus.kyoto-u.ac.jp.

[1] The abbreviations used are: NF-κB, nuclear factor-κB; TNFα, tumor necrosis factor-α; TAD, transactivation domain; CREB, cAMP response element-binding protein; CBP, cAMP response element-binding protein-binding protein; CPAP, centrosomal P4.1-associated protein; STAT, signal transducer and activator of transcription; GST, glutathione *S*-transferase; siRNA, small interfering RNA; DBD, DNA-binding domain; SRC-1, steroid receptor coactivator-1; C/H, cysteine/histidine-rich.

RelA as well as CBP and functions as a scaffolding protein by tethering together the RelA-CBP-BRCA1 complex, thereby supporting the transacting function of CBP (21).

Thus, not only TAD, but also the N-terminal region of RelA appears to contribute to NF-κB target gene induction. However, little is known about the factors that interact with the N-terminal region. Here, we sought to clarify the mechanism of NF-κB-dependent transcriptional activation by identifying factors that interact with the N-terminal region of RelA. In a yeast two-hybrid screen using the N terminus of RelA as bait, we identified a novel RelA-interacting factor, centrosomal P4.1-associated protein (CPAP). CPAP was previously identified by virtue of its interaction with the cytoskeletal protein 4.1R-135 (22). Although CPAP appears to be a component of the centrosomal complex, the majority of CPAP is found in soluble fractions, mainly in the cytoplasm and a small portion in the nucleus (22, 23). In addition, it was previously reported that CPAP interacts with STAT5 and enhances STAT5-mediated transcription (23), although the mechanism by which this occurs remains unclear. In this study, we show evidence suggesting that CPAP is a novel coactivator of NF-κB that binds to the N-terminal region of RelA, possibly activating transcription through CBP.

EXPERIMENTAL PROCEDURES

Plasmid Construction—pEFr-FLAG-CPAP was a kind gift from Dr. J. E. Visvader (Walter and Eliza Hall Institute of Medical Research, Melbourne, Australia) (23). The cDNA fragment consisting of the entire open reading frame of CPAP was generated by PCR using a human spleen cDNA library (Clontech, Palo Alto, CA) as the template and primers 5′-CGCGGATCCATGTTCCTGATGCCAACCTC-3′ and 5′-TTTTCCTTTTGCGGCC GCATCGTCACAGCTCCGTGTCC-3′. The fragment was inserted into the BamHI-NotI sites of the pcDNA3-Myc vector (24) to construct pcDNA3-Myc-CPAP and blunt-end cloned into the pCMV-FLAG vector (24) to generate pCMV-CPAP. The series of plasmids encoding deletion mutants of CPAP, pcDNA3-Myc-CPAP-(1–1149), pcDNA3-Myc-CPAP-(1150–1338), and pcDNA3-Myc-CPAP-(967–1338), was constructed by inserting fragments generated by PCR using appropriate synthetic oligonucleotides as primers and pcDNA3-Myc-CPAP as the template. pcDNA3-HA-RelA (where HA is hemagglutinin), pcDNA3-HA-RelA-(1–427), pcDNA3-HA-RelA-(428–551), pcDNA3-HA-RelA-(1–312), pcDNA3-HA-RelA-(313–427), and pcDNA3-HA-RelA-(201–427) were generated in a similar manner using pcDNA3-RelA (25) as the template.

pGEX-2TK-RelA was created by inserting the RelA BamHI-MfeI fragment into the BamHI-EcoRI sites of the pGEX-2TK vector (Clontech). pFastBac1-RelA was constructed by inserting the glutathione *S*-transferase (GST)-RelA fragment of pGEX-2TK-RelA into the BamHI-XbaI sites of the pFastBac1 vector (Invitrogen). pGEX-CPAP-C was created by inserting the EcoRI-NotI fragment of pcDNA3-Myc-CPAP-(967–1338) into the EcoRI-NotI sites of the pGEX-6P-1 vector (Clontech).

pM-CPAP was generated by inserting the BamHI-XbaI fragment, which was PCR-amplified from pcDNA3-Myc-CPAP using primers 5′-CGCGGATCCCAATGTTCCTGATGCCAACCTC-3′ and 5′-GCTCTAGAATCGTCACAGCTCCGTGTCC-3′, into the BamHI-XbaI sites of the pM vector (Clontech). pM-CPAP-(967–1338) was obtained by inserting the EcoRI-XbaI fragment of pcDNA3-Myc-CPAP-(967–1338) into the EcoRI-XbaI sites of the pM vector.

pCMV-CBP was a kind gift from Dr. I. Talianidis (Institute of Molecular Biology and Biotechnology, Crete, Greece) (26). The expression plasmids for a series of CBP deletion mutants (CBP1–CBP5) were kindly provided by Dr. A. Fukamizu (Center for Tsukuba Advanced Research Alliance, Tsukuba, Japan) (27). The reporter plasmids pNF-κB-luc and pFR-luc were obtained from Stratagene. The construction of the reporter plasmid pNF-κB-mt-luc was described previously (28).

Yeast Two-hybrid Screening—The DNA fragment encoding amino acids 1–427 of RelA was subcloned into the pHybLex-Zeo vector (Invitrogen). This plasmid was used as a bait construct to screen a human leukemia cDNA library (Clontech) according to the manufacturer's instructions (Invitrogen). A total of 1.6×10^6 transformants were selected based on histidine prototrophy and β-galactosidase activity.

GST Pull-down Assay—GST and the GST-RelA fusion protein, encoded by pFastBac1 and pFastBac1-RelA, respectively, were produced in Sf9 cells using the Bac-to-Bac baculovirus expression system (Invitrogen). GST and the GST-CPAP-(967–1338) fusion protein, encoded by pGEX-6P-1 and pGEX-CPAP-(967–1338), respectively, were produced in BL21 cells (Amersham Biosciences) exposed to 0.1 mM isopropyl β-D-thiogalactopyranoside. After affinity separation of the proteins from cell lysates using glutathione-Sepharose (Amersham Biosciences), proteins bound to the resin were mixed and incubated with *in vitro* transcription/translation products at 4 °C for 2 h. The *in vitro* transcription/translation product was prepared with the TnT T7 quick coupled transcription/translation system (Promega) using 0.25 μg of each expression plasmid in the presence of L-[^{35}S]methionine (Amersham Biosciences) according to the manufacturer's instructions. After being washed five times in binding buffer (50 mM Tris-HCl (pH 8.0), 150 mM NaCl, 1 mM EDTA, 0.5% Nonidet P-40, 1 mM dithiothreitol, and 1 mM phenylmethylsulfonyl fluoride), resin-bound radiolabeled proteins were fractionated by SDS-PAGE and detected by autoradiography.

Cell Culture and Transfection—293T and MCF-7 cells were cultured in Dulbecco's modified Eagle's medium (Nissui) supplemented with 10% fetal bovine serum and L-glutamine. Transfection of plasmids into cells was performed with FuGENE 6 transfection reagent (Roche) according to the manufacturer's recommendations.

Immunoprecipitation—Cells were lysed in immunoprecipitation buffer (50 mM Tris-HCl (pH 7.5), 150 mM NaCl, and 0.1% Nonidet P-40). After centrifugation, the supernatant was incubated with anti-FLAG antibody M2 (Sigma), anti-RelA antibody F-6 (Santa Cruz Biotechnology, Inc.), anti-c-Myc antibody 9E10 (Santa Cruz Biotechnology, Inc.), or normal mouse IgG (Zymed Laboratories Inc.) for at least 1 h. Immunocomplexes were recovered by adsorption to protein G-Sepharose (Amersham Biosciences). After being washed five times in immunoprecipitation buffer, the immunoprecipitates were analyzed by immunoblotting.

Immunoblot Analysis—Immunoblot analysis was performed essentially as described previously (29). The antibodies used in these experiments were specific for FLAG, RelA (antibody F-6), and α-tubulin (antibody-1, Calbiochem). The rabbit antiserum against CPAP was kindly provided from Dr. T. K. Tang (Institute of Biomedical Sciences, Taipei, Taiwan, Republic of China) (22).

Reporter Assay—Cell extracts were prepared in reporter lysis buffer (Promega) 48 h after transfection. After removal of cell debris, the luciferase activity in the extracts was measured with a luciferase assay kit (Promega) and a Berthold Lumat LB 9507 luminometer according to the manufacturers' instructions.

RNA Interference Technique—A 21-nucleotide small interfering RNA (siRNA) duplex (5′-AAUGGAAUGCACGUGACGAUG-3′) containing 3′-dTdT overhanging sequences was synthesized (Qiagen Inc.). siRNA transfection was performed using Oligofectamine reagent (Invitrogen) according to the manufacturer's instructions.

RNA Isolation and Reverse Transcription-PCR—Total RNA was isolated from cultured cells using Sepasol RNA I Super (Nacalai Tesque, Kyoto, Japan) according to the manufacturer's instructions. The relative expression of each mRNA was evaluated by semiquantitative reverse transcription-PCR using a One-Step RNA PCR kit (Takara). Glyceraldehyde-3-phosphate dehydrogenase mRNA was used as an internal control. The primers used were as follows: CPAP, 5′-AAAGGGACCACAGGTAGCGG-3′ and 5′-TGAATTCACTCGCACGATCTGGGATG; interferon-β, 5′-CACGACAGCTCTTTCCATGA-3′ and 5′-AGCCAGTGCTCGATGAATCT-3′; and TNF receptor-associated factor-1, 5′-GCCCCTGATGAGAATGAGTT-3′ and 5′-CTCATGCTCTTGCACAGACT-3′.

Indirect Immunofluorescence Analysis—Indirect immunofluorescence analysis was performed as described previously (29). Cells were permeabilized with 0.05% Triton X-100 after fixation and treated with anti-RelA primary antibody F-6 or rabbit antiserum against CPAP (22). Secondary antibodies conjugated to Alexa 488 and Alexa 568 (Molecular Probes, Inc.) were used to visualize primary antibody distribution. Nuclei were stained with 4′,6-diamidino-2-phenylindole (Sigma).

DNA-Protein Complex Immunoprecipitation Assay—293T cells treated with 10 nM TNFα were transfected with plasmids. After crosslinking with 1% formaldehyde for 15 min, cells were lysed; sonicated; and subjected to immunoprecipitation using anti-FLAG or anti-RelA antibody or normal mouse IgG. Recovered immunocomplexes were incubated at 65 °C for 16 h and then digested with proteinase K for 2 h. DNA was extracted from the immunocomplexes with phenol and precipitated with ethanol. The primers used for detection of recovered DNA were 5′-ACCGAAACGCGCGAGGCAGGATCAGCCATA-3′ and 5′-GCTCTCCAGCGGTTCCATC-3′ for pNF-κB-luc and 5′-CTAGCAAAATAGGCTGTCCC-3′ and 5′-CTTTATGTTTTTGGCGTATTCCA-3′ for pNF-κB-mt-luc.

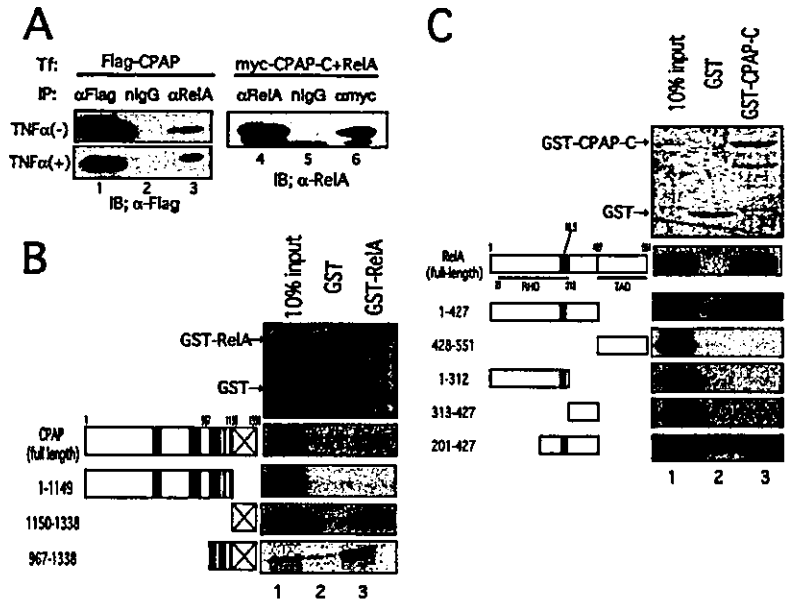

FIG. 1. **Interaction between RelA and CPAP.** *A*, interaction between RelA and full-length CPAP without (*left upper panel*) and with (*left lower panel*) TNFα stimulation or the C-terminal domain of CPAP from amino acids 967 to 1338 (CPAP-C) (*right panel*). Lysates from 293T cells transfected with 10 μg of pEFr-FLAG-CPAP or 8 μg of pcDNA3-Myc-CPAP-C and 2 μg of pcDNA3-RelA were used for the immunoprecipitation analysis. *Tf* and *IP* denote proteins produced from the transfected plasmids and antibodies used in the immunoprecipitation experiments, respectively. *αFLAG*, *nIgG*, *αRelA*, and *αmyc* indicate anti-FLAG antibody, normal mouse IgG, anti-RelA antibody, and anti-Myc antibody, respectively. FLAG-tagged CPAP and RelA in the immunoprecipitates were detected by immunoblotting (*IB*) using anti-FLAG and anti-RelA antibodies, respectively. *B*, mapping of the region of CPAP responsible for interaction with RelA by deletion analysis. The ^{35}S-labeled *in vitro* transcription/translation product of full-length CPAP or its deletion mutants was incubated with GST (*lane 2*) or GST-RelA (*lane 3*) immobilized on glutathione-Sepharose. The proteins bound to the resin were eluted, resolved by SDS-PAGE, and visualized by autoradiography (*lower panel*). *10% input* indicates 0.1 volume of the ^{35}S-labeled product used in the pull-down assay (*lane 1*). The Coomassie Brilliant Blue staining pattern of proteins pulled down from the reaction mixture containing full-length CPAP is shown as an example (*upper panel*). Bands representing GST and GST-RelA are indicated by *arrows*. A schematic representation of the structures of CPAP and its deletion mutants is shown on the left. CPAP contains a leucine zipper motif (*gray boxes*), a series of nonamer glycine repeats (G-box region; *crossed boxes*), three putative nuclear localization signals (*dashed boxes*), and two potential nuclear export signals (*black boxes*). The *numbers* indicate the amino acids demarcating fragments of the CPAP protein used. *C*, mapping of the RelA region that interacts with CPAP by deletion analysis. The ^{35}S-labeled product of full-length RelA or its truncated mutants was incubated with GST (*lane 2*) or GST-CPAP-C (*lane 3*). The Coomassie Brilliant Blue staining pattern of proteins pulled down from the reaction mixture with full-length RelA is shown as an example (*upper panel*). The bands representing GST and GST-CPAP-C are indicated by *arrows*. A schematic representation of RelA and its mutants is shown on the left. RelA contains a Rel homology domain (*RHD*), a nuclear localization signal (*NLS*), and a TAD.

RESULTS

Identification of CPAP as a Factor That Interacts with RelA—To identify cellular factors that interact with the N-terminal region of RelA, a yeast two-hybrid screen was performed using a human leukemia cDNA library as bait and the N-terminal 427-amino acid region of RelA as prey. From 1.6 × 10^6 L40 yeast transformants, 64 clones were obtained that appeared to interact with RelA. Among them, three independent clones were revealed to encode portions of CPAP.

To confirm the interaction of CPAP with RelA, we performed an immunoprecipitation assay using 293T cells exogenously producing FLAG-tagged CPAP. FLAG-tagged CPAP was detected in cell lysates in the immunocomplex formed with anti-RelA antibody (Fig. 1*A*, *left panels*, *lane 3*), but not with normal IgG (*lane 2*). The interaction between FLAG-tagged CPAP and endogenous RelA was seen without considerable alteration both before and after treatment with TNFα (Fig. 1*A*, *upper* and *lower left panels*, respectively). This seemed to imply that TNFα-induced phosphorylation of RelA is not essential for the interaction with CPAP. Actually, we found that FLAG-tagged CPAP was co-immunoprecipitated with a RelA mutant in which one of the TNFα-induced phosphorylation target sites (Ser^{276}) was replaced with alanine (data not shown). This may support the above idea. This interaction was also seen in a GST pull-down assay. Under conditions in which *in vitro* translated CPAP was not pulled down with GST-bound Sepharose beads (Fig. 1*B*, *lane 2*), we found it in a pellet with recombinant GST-RelA-bound Sepharose beads (*lane 3*). These results suggest that CPAP interacts specifically with RelA. In addition, to examine the region of CPAP responsible for interaction with RelA, we performed a GST pull-down assay as described above using several deletion mutants of CPAP. The *in vitro* synthesized fragments of CPAP spanning amino acids 1150–1338 and 967–1338, but not amino acids 1–1149, were co-purified with GST-RelA (Fig. 1*B*). This indicates that the region of CPAP responsible for interaction with RelA resides within amino acids 1150–1338, including a series of 21 nonamer repeats (G-box region). This result was also obtained with the immunoprecipitation assay. In the lysates of 293T cells producing RelA and Myc-tagged CPAP-C (C-terminal amino acids 967–1338 of CPAP), exogenous RelA was efficiently detected in immunocomplexes formed with anti-Myc antibody (Fig. 1*A*, *right panel*, *lane 6*), but not with normal mouse IgG (*lane 5*). The region of RelA that interacts with CPAP was similarly assessed. The *in vitro* synthesized fragments of RelA spanning amino acids 1–427 and 201–427, but not amino acids 428–551, 1–312, or 313–427, were co-purified with GST-CPAP-C (Fig. 1*C*). These results indicate that the central region of RelA is necessary and sufficient for interaction with CPAP.

CPAP Augments NF-κB-dependent Gene Expression—Because CPAP has been reported to activate STAT5-mediated transcription (23), we examined the effect of this protein on RelA-mediated transcription using a reporter assay. When CPAP was ectopically expressed, NF-κB-responsive reporter gene expres-

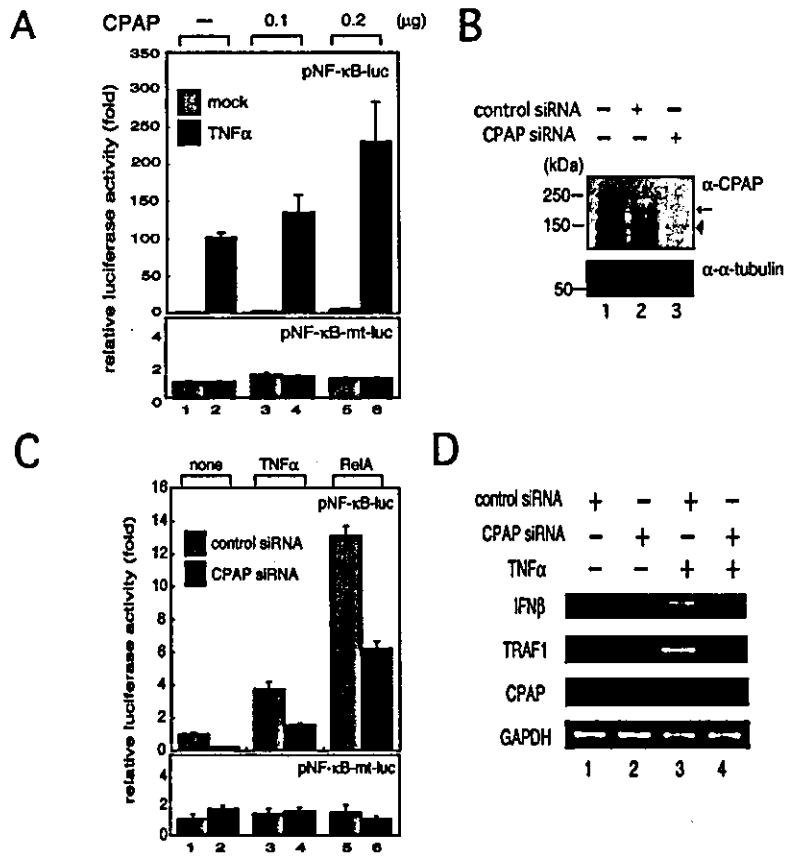

FIG. 2. **CPAP increases NF-κB-induced gene expression.** *A*, enhancement of NF-κB-dependent reporter gene expression by ectopic expression of CPAP. 293T cells were transfected with 25 ng of pNF-κB-luc (containing wild-type NF-κB-binding sites upstream of the luciferase gene; *upper panel*) or pNF-κB-mt-luc (containing mutated NF-κB-binding sites; *lower panel*) together with the indicated amounts of pCMV-FLAG-CPAP. After 42 h of transfection, cells were mock-treated (*bars 1*, *3*, and *5*) or treated with 10 ng/ml TNFα (*bars 2*, *4*, and *6*) and harvested after an additional incubation for 6 h. Values represent the relative luciferase activity expressed as the mean ± S.E. of three independent transfections. *B*, suppression of endogenous CPAP production by siRNA. The 21-nucleotide RNA duplex (siRNA) directed against the CPAP sequence was transfected into MCF-7 cells (*lane 1*). The levels of CPAP protein were evaluated by immunoblotting 48 h post-transfection. As a negative control, total cell extracts from MCF-7 cells with no siRNA treatment (*lane 1*) and with treatment with control siRNA (*lane 2*) were used. The relative protein levels of CPAP (*upper panel*) and α-tubulin as a positive control (*lower panel*) are shown. Molecular mass markers are shown on the left. The *arrow* indicates intact CPAP protein. The *arrowhead* shows the putative degraded form of CPAP. *C*, effects of CPAP siRNA on NF-κB-dependent reporter gene expression. MCF-7 cells were transfected with control siRNA (*gray bars*) or CPAP siRNA (*black bars*). At 24 h post-transfection, 25 ng of pNF-κB-luc, 25 ng of pRL-TK-luc, and 200 ng of either pKS$^+$-CMV (*bars 1–4*) or pcDNA3-RelA (*bars 5* and *6*) were transfected into cells (*upper panel*). The same experiment using pNF-κB-mt-luc instead of pNF-κB-luc was also carried out (*lower panel*). An additional 18 h later, cells were treated with (*bars 3* and *4*) or without (*bars 1*, *2*, *5*, and *6*) 10 ng/ml TNFα for 6 h. Values represent the luciferase activity expressed as the mean ± S.E. of three independent transfections. *D*, effects of CPAP siRNA on endogenous gene expression induced by TNFα. MCF-7 cells were transfected with control (*lanes 1* and *3*) or CPAP siRNA (*lane 2* and *4*). The cells were treated for 6 h with 10 ng/ml TNFα (*lanes 3* and *4*). Semiquantitative reverse transcription-PCR was performed to estimate the amounts of interferon-β (*IFNβ*), TNF receptor-associated factor-1 (*TRAF1*), CPAP, and glyceraldehyde-3-phosphate dehydrogenase (*GAPDH*) mRNAs.

sion was enhanced by up to 2–3-fold in a dose-dependent manner (Fig. 2*A*, *upper panel*). In contrast, reporter activity from the plasmid containing mutated NF-κB-binding sites in the promoter region was not affected by ectopically expressed CPAP (Fig. 2*A*, *lower panel*). These data suggest that CPAP can specifically up-regulate NF-κB-mediated transcription.

To investigate the contribution of endogenous CPAP to transcriptional activation, we examined the effect of CPAP siRNA, which was designed to specifically knock down the expression of CPAP, on NF-κB-dependent transcriptional activation in MCF-7 breast cancer-derived cells. We confirmed that endogenous CPAP protein levels were significantly reduced by transfection with CPAP siRNA, whereas the levels of other cellular proteins such as α-tubulin were not changed (Fig. 2*B*). The level of NF-κB-mediated transcription induced by either TNFα or RelA in CPAP siRNA-treated cells was decreased to <50% of that in cells transfected with control siRNA (Fig. 2*C*, *upper panel*). In contrast, reporter activity from the plasmid containing mutated NF-κB-binding sites was not affected by knocking down CPAP (Fig. 2*C*, *lower panel*). These findings indicate that endogenous CPAP is required for full activation of NF-κB-dependent reporter gene expression.

Next, we examined whether CPAP affects expression of endogenous target genes. After treatment with TNFα, total RNA was isolated from MCF-7 cells transfected with either control or CPAP siRNA and analyzed by reverse transcription-PCR to detect the mRNA levels of interferon-β and TNF receptor-associated factor-1, which are known to be induced by NF-κB. As shown in Fig. 2*D*, transfection with CPAP siRNA, but not control siRNA, down-regulated TNFα-induced expression of interferon-β and TNF receptor-associated factor-1 mRNAs. These results indicate that CPAP plays an important role in NF-κB-mediated transcriptional activation in cells.

Translocation of CPAP into the Nucleus upon TNFα Treatment—RelA is translocated from the cytoplasm into the nucleus upon stimulation by specific cytokines. To determine

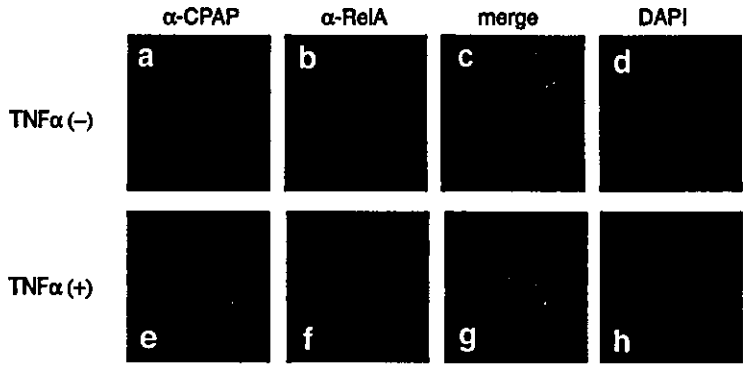

FIG. 3. **The subcellular localization of CPAP is partially shifted from the cytoplasm to the nucleus by TNFα stimulation.** Indirect immunofluorescence analysis was performed on MCF-7 cells treated with (*lower panels*) or without (*upper panels*) TNFα for 20 min. The antibodies used in this experiment were anti-CPAP (*α-CPAP*; *a* and *e*, *green*) and anti-RelA (*α-RelA*; *b* and *f*, *red*). Merged images of *green* and *red* signals are shown (*c* and *g*). 4′,6-Diamidino-2-phenylindole (*DAPI*) was used to visualize nuclear staining (*d* and *h*).

whether the localization of CPAP is similarly altered by activation of the NF-κB pathway, we examined the subcellular localization of CPAP in MCF-7 cells by indirect immunofluorescence analysis with or without TNFα treatment. As reported previously (23), CPAP was found to localize primarily in the cytoplasm, although some protein was also detectable in the nucleus without stimulation (Fig. 3*a*). As CPAP was immunoprecipitated with RelA from the cytoplasmic fraction of such cells (data not shown), it seemed likely that a cytoplasmic complex is present before TNFα treatment. However, following TNFα treatment for 20 min, a portion of CPAP was observed to accumulate in the nucleus (Fig. 3*e*), similar to RelA (*b* and *f*). These results suggest that at least a portion of cytoplasmic CPAP enters the nucleus in a TNFα-dependent manner.

Recruitment of CPAP to the NF-κB-binding Motif—The increase in NF-κB-dependent transcriptional activation by CPAP, the nuclear accumulation of CPAP in response to TNFα stimulation, and the physical interaction of CPAP with RelA all suggested the possibility that CPAP, together with RelA, is recruited to the transcriptional promoters of NF-κB target genes. To examine this possibility, we performed a DNA-protein complex immunoprecipitation assay. As shown in Fig. 4 (*upper panel, lanes 1–3*), a DNA fragment containing an NF-κB-binding motif was detected by PCR in complexes specifically immunoprecipitated by either anti-FLAG or RelA antibodies from lysates of 293T cells transfected with pNF-κB-luc, FLAG-tagged CPAP, and RelA expression plasmids. In contrast, no DNA fragment was amplified from cells transfected with pNF-κB-mt-luc instead of pNF-κB-luc (Fig. 4, *lower panel, lanes 2* and *3*). These data suggest that CPAP is recruited to the transcriptional promoter region containing an NF-κB-binding motif via association with RelA.

CPAP Can Activate Gene Expression When Tethered to a Transcriptional Promoter—We showed above that CPAP interacted with RelA, up-regulated NF-κB-mediated transcription, and formed part of the complex binding to a transcriptional promoter containing NF-κB-binding motifs. These data suggest that CPAP acts as a transcriptional coactivator of NF-κB. We examined this possibility using a one-hybrid assay system with fusion proteins consisting of the Gal4 DNA-binding domain (DBD) and full-length CPAP or its C-terminal region in mammalian cells. As demonstrated in Fig. 5 (*second bar*), Gal4 DBD-fused CPAP up-regulated luciferase expression from pFR-luc, a reporter plasmid containing a Gal4-responsive transcriptional promoter. In contrast, CPAP by itself had no effect on the same promoter (Fig. 5, *third bar*). No difference in luciferase levels was observed among the exogenous Gal4 DBD-containing constructs (data not shown). This suggests that

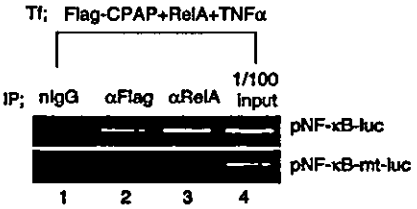

FIG. 4. **Recruitment of CPAP to a promoter containing an NF-κB-binding motif.** 293T cells cotransfected with expression plasmids for RelA and FLAG-CPAP and pNF-κB-luc (*upper panel*) or pNF-κB-mt-luc (*lower panel*) were harvested after treatment with TNFα for 20 min. After formaldehyde fixation, the cross-linked DNA-protein complexes were immunoprecipitated with anti-RelA antibody (*αRelA*; *lane 3*), anti-FLAG antibody (*αFLAG*; *lane 2*), or normal mouse IgG (*nIgG*; *lane 1*). 1% input of total cell lysate was used as positive control (*lane 4*). The DNA extracted from each immunoprecipitate was used as the template for PCR to detect the DNA fragment containing NF-κB-binding motifs as described under "Experimental Procedures." *Tf* and *IP* denote proteins produced from the transfected plasmids and antibodies used in the immunoprecipitation experiments, respectively.

CPAP has a transactivation capacity when tethered to the transcriptional promoter. This activity is likely to be located in the C-terminal part of CPAP because this region showed higher reporter activation compared with full-length CPAP (Fig. 5, *fourth* and *second bars*, respectively). Together with our results above, these data suggest that CPAP acts as a transcriptional coactivator in the NF-κB transcriptional complex.

Interaction between CPAP and CBP—To obtain insights into the mechanism of CPAP-dependent transcriptional activation, we assessed whether CPAP can recruit known coactivators to the transcriptional promoter. First, we examined the physical association of CPAP with CBP, p300, steroid receptor coactivator-1 (SRC-1), and transcription intermediary factor-2 using a GST pull-down assay. *In vitro* synthesized CBP or p300, but not SRC-1 or transcription intermediary factor-2, was co-purified with GST-CPAP-C, whereas none could be pulled down by GST itself (Fig. 6*A*) (data not shown), suggesting that CPAP interacts with CBP and p300. To narrow down the region of CBP required for interaction with CPAP, deletion analysis was carried out using five CBP fragments, CBP1–CBP5 (27), which were produced and metabolically labeled in cells. Only CBP4, which contains the C/H3 domain, could be co-purified with GST-CPAP-C (Fig. 6*B*), suggesting that CPAP associates with CBP through this region of CBP.

Next, we performed a reporter assay to examine the effect of CPAP on NF-κB-mediated transcription. As shown in Fig. 6*C*, overexpression of either CBP or CPAP in cells enhanced TNFα-induced NF-κB-dependent transcription by ~2–3-fold

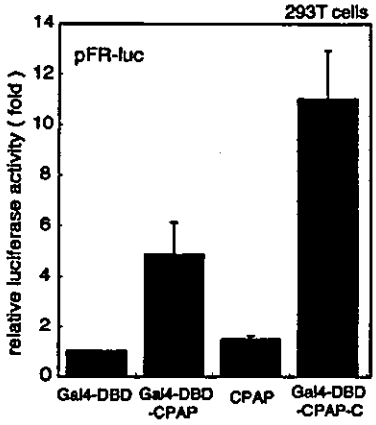

FIG. 5. **CPAP supports transcriptional activation when tethered to the promoter.** 293T cells were transfected with 50 ng of pFR-luc together with 0.3 μg of pM, pM-CPAP, pCMV-FLAG-CPAP, or pM-CPAP-C. After 48 h of transfection, cells were harvested and subjected to a luciferase assay. Values represent the relative luciferase activity expressed as the mean ± S.E. of three independent transfections.

compared with untransfected cells. When both CBP and CPAP were overexpressed in cells, reporter gene expression was synergistically elevated to levels 10-fold higher than in untransfected cells. These results suggest that CPAP contributes to NF-κB-dependent transcriptional activation at least partly by binding CBP and recruiting it to the cellular transcriptional machinery.

DISCUSSION

We identified CPAP as a molecule that associates with RelA and contributes to RelA-mediated transcriptional activation. Although CPAP was previously identified as a centrosomal protein (22), its function was not clear. Recently, however, CPAP was reported to interact with STAT5 to enhance STAT5-mediated transcription (23). However, the mechanism of CPAP-mediated transcriptional activation remained unclear. In this study, we have presented data showing that CPAP is a component of the NF-κB transcriptional activation complex and can activate transcription when tethered to a promoter. Moreover, we found that the transcriptional coactivator CBP contributes at least in part to transcriptional activation by association with CPAP.

Because CPAP fused with Gal4 DBD, but not CPAP itself, could induce reporter gene expression under the control of a promoter with Gal4-responsive elements (Fig. 5), CPAP is likely to activate transcription when presented to the transcriptional machinery. We also observed that CPAP exists in a DNA-protein complex including RelA and an NF-κB-responsive element, suggesting that CPAP binds to the promoter of NF-κB target genes in association with RelA to activate transcription. Enhancement of STAT5-mediated transcription by CPAP could be explained by a similar mechanism because CPAP was shown to interact with STAT5a/b as well as RelA. These data suggest that CPAP is a transcriptional coactivator.

The C-terminal 372 amino acids of CPAP exhibited transcriptional activation capability when fused with Gal4 DBD, suggesting that this region is responsible for transcriptional activation. This region associates with CBP, indicating that CBP may be involved in the transcriptional activation potential of CPAP. CBP is known to activate transcription by two mechanisms. CBP functions as a molecular bridge between the basal transcriptional machinery and transcription factors recruited to specific enhancer elements. In addition, the histone acetyltransferase activity of CBP plays an essential role in opening up chromatin structure to allow for efficient transcriptional activity (30, 31). Previous work also showed that p300/CBP binds to RelA and supports NF-κB-mediated transcriptional activation (9, 10). Here, we have shown that CPAP can associate with p300/CBP as well as RelA, indicating that these three proteins may form a complex. The breast cancer-related BRCA1 has been proposed to function as a scaffolding protein that tethers several factors, including RelA, CBP, and RNA polymerase II, to transcriptional promoter elements (21). By analogy with BRCA1, it seems likely that CPAP supports the transactivating effects of CBP by acting as a scaffolding protein that stabilizes CBP within the NF-κB transcriptional complex. We have shown that the C-terminal domain of CPAP interacts with the C-terminal region of p300/CBP containing the C/H3 and glutamine-rich domains. It was previously reported that the C-terminal TAD of RelA interacts mainly with the N-terminal region of p300/CBP containing the C/H1 and KIX domains (9, 10), which is distinct from the region that interacts with CPAP. These results may provide a structural framework for the formation of a complex including these three factors. However, the interactions are likely rather more complex because the C-terminal region of CPAP has also been identified as a RelA-interacting region. Furthermore, we already found that CPAP forms multimer (data not shown). Therefore, stoichiometric analysis will be required to unveil the functional structure of this mysterious complex as well as to better understand the molecular mechanism of CPAP-dependent transcriptional activation.

It is well known that some CBP-associated transcriptional coactivators such as p300/CBP-associated factor, SRC-1, and ACTR have histone acetyltransferase activity (32–34). Some members of the p300/CBP-associated factor-related family with strong histone acetyltransferase activity, such as GCN5, have a conserved amino acid sequence called motif A (35), which is considered to be a characteristic structural feature of histone acetyltransferase. However, we have not found any amino acid sequences similar to motif A in CPAP. On the other hand, it has been reported that the histone acetyltransferase domains of SRC-1 and ACTR members of the SRC family with relatively low histone acetyltransferase activity share regions of high glutamine content (33, 34). Because CPAP has multiple glycine or glutamine repeats in the C-terminal region shown to have transcriptional activation capacity, it is possible that CPAP possesses histone acetyltransferase activity in the C-terminal region. To determine whether this is in fact the case, biochemical analysis using purified CPAP is required in the future.

Besides functioning as a transcriptional coactivator, CPAP might also affect interactions between RelA and molecules that inhibit NF-κB-mediated transcription, such as IκB, histone deacetylase-1 (13), and RelA-associated inhibitor (36). Histone deacetylase-1 has been reported to interact directly with the N-terminal region of RelA to exert its corepressor function (13). RelA-associated inhibitor, which binds to the central region of RelA, has also been reported to inhibit RelA-mediated transcriptional activation via an unknown mechanism (36). As we have already detected that IκBα was coprecipitated with a CPAP-RelA complex from the cell lysate (data not shown), it may be unlikely that the presence of IκBα precludes the association of RelA and CPAP. Further analysis of the complex including RelA and CPAP under physiological conditions should provide valuable insight into the regulatory mechanism of NF-κB-dependent transcriptional activation.

In addition, we found that the subcellular localization of CPAP was partially altered from the cytoplasm to the nucleus upon TNFα treatment. It was also previously reported that CPAP, which binds to STAT5, translocates from the cytoplasm

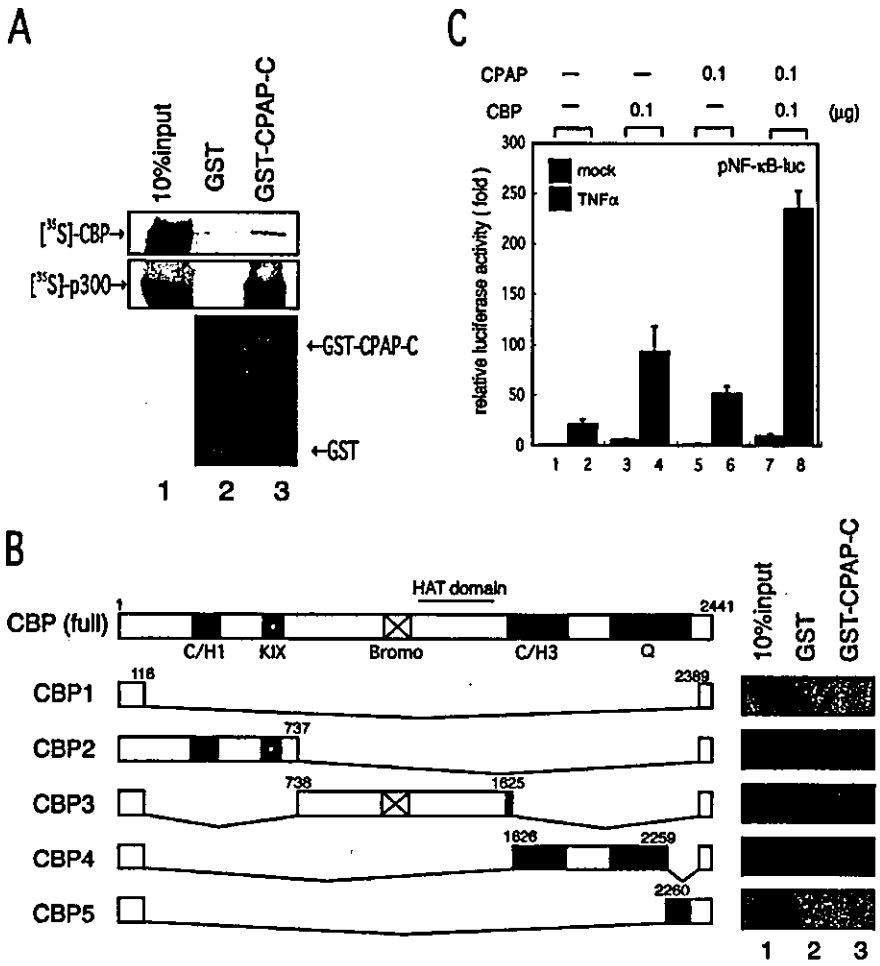

FIG. 6. **Association between CPAP and CBP.** *A*, results from a GST pull-down assay performed as described under "Experimental Procedures." ^{35}S-Labeled full-length CBP (*upper panel*) or p300 (*middle panel*) was incubated with recombinant GST (*lane 2*) or GST-CPAP-C (*lane 3*). *10%input* indicates 0.1 volume of the ^{35}S-labeled product used in the pull-down assay (*lane 1*). The Coomassie Brilliant Blue staining pattern of GST fusion proteins is shown (*lower panel*). *B*, mapping of the region of CBP that interacts with CPAP by deletion analysis. A schematic representation of the structures of CBP and its deletion mutants (CBP1–CBP5) is shown on the left. *Numbers* above the diagrams indicate the amino acid positions of CBP relative to the N terminus. C/H1 and C/H3 are the cysteine/histidine-rich regions, and KIX is the CREB-binding domain. *Bromo*, bromodomain; *Q*, glutamine-rich domain. The results of the GST pull-down assay using the C-terminal region of CPAP and a series of deletion mutants of CBP are shown on the right. ^{35}S-Labeled CBP1–CBP5 were incubated with recombinant GST (*lane 2*) or GST-CPAP-C (*lane 3*). *HAT*, histone acetyltransferase. *C*, synergistic enhancement of NF-κB-dependent reporter gene expression by CPAP and CBP. 293T cells were transfected with 25 ng of pNF-κB-luc together with the indicated amounts of pCMV-FLAG-CPAP (*CPAP*; *bars 5–8*) and/or pCMV-CBP (*CBP*; *bars 3, 4, 7,* and *8*). After 42 h of transfection, cells were treated with (*black bars 2, 4, 6,* and *8*) or without (*mock*; *gray bars 1, 3, 5,* and *7*) 10 ng/ml TNFα and harvested after an additional incubation for 6 h. Values represent the luciferase activity expressed as the mean ± S.E. of three independent transfections.

to the nucleus in response to prolactin-mediated activation of the JAK-STAT pathway and enhances STAT5-dependent transcription (23). As it has been reported that CPAP has three putative nuclear localization signals in its C-terminal region (23), it seems possible that CPAP is retained in the cytoplasm somehow in the steady state of cells, but released by particular stimuli. It has been revealed that ACTR, which is located mainly in the cytoplasm with a small portion in the nucleus in most cells, translocates from the cytoplasm to the nucleus upon TNFα activation and subsequent phosphorylation by IκB kinase-β (37). Further study on the molecular mechanism of stimulation-dependent nuclear translocation of CPAP may provide new knowledge regarding the fine regulation of gene expression by extracellular stimuli.

In this study, we have shown that CPAP can modulate RelA function in the nucleus. However, CPAP was first identified as a component of the centrosomal complex. The molecular interaction between CPAP and RelA evokes the possibility that RelA exists in centrosomes. Centrosomal location of factors related to transcription, such as p53 (38, 39) and BRCA1 (40, 41), has been reported and may be involved in centrosomal replication in a transcriptional activity-dependent or -independent manner. Further analysis of whether the interaction between CPAP and RelA affects centrosomal function may reveal new biological roles for RelA as well as CPAP.

Acknowledgments—We thank Dr. J. E. Visvader for providing pEFr-FLAG-CPAP, Dr. T. K. Tang for rabbit antiserum against CPAP, Dr. I. Thlianidis for pCMV-CBP, and Dr. A. Fukamizu for CBP deletion mutants. We thank M. Matsumoto-Kadowaki for help with confocal microscopy and Dr. T. Ohshima, T. Ego, Y. Miyanari, and others at our institute for helpful comments and discussions.

REFERENCES

1. Baldwin, A. S., Jr. (1996) *Annu. Rev. Immunol.* **14**, 649–683
2. Ghosh, S., May, M. J., and Kopp, E. B. (1998) *Annu. Rev. Immunol.* **16**, 225–260
3. Karin, M., Cao, Y., Greten, F. R., and Li, Z. W. (2002) *Nat. Rev. Cancer* **2**, 301–310

4. Chen, L. F., and Greene, W. C. (2004) *Nat. Rev. Mol. Cell. Biol.* **5,** 392–401
5. Schmitz, M. L., Stelzer, G., Altmann, H., Meisterernst, M., and Baeuerle, P. A. (1995) *J. Biol. Chem.* **270,** 7219–7226
6. Yamit-Hezi, A., and Dikstein, R. (1998) *EMBO J.* **17,** 5161–5169
7. Yamit-Hezi, A., Nir, S., Wolstein, O., and Dikstein, R. (2000) *J. Biol. Chem.* **275,** 18180–18187
8. Uranishi, H., Tetsuka, T., Yamashita, M., Asamitsu, K., Shimizu, M., Itoh, M., and Okamoto, T. (2001) *J. Biol. Chem.* **276,** 13395–13401
9. Gerritsen, M. E., Williams, A. J., Neish, A. S., Moore, S., Shi, Y., and Collins, T. (1997) *Proc. Natl. Acad. Sci. U. S. A.* **94,** 2927–2932
10. Zhong, H., Voll, R. E., and Ghosh, S. (1998) *Mol. Cell* **1,** 661–671
11. Sheppard, K. A., Rose, D. W., Haque, Z. K., Kurokawa, R., McInerney, E., Westin, S., Thanos, D., Rosenfeld, M. G., Glass, C. K., and Collins, T. (1999) *Mol. Cell. Biol.* **19,** 6367–6378
12. Werbajh, S., Nojek, I., Lanz, R., and Costas, M. A. (2000) *FEBS Lett.* **485,** 195–199
13. Zhong, H., May, M. J., Jimi, E., and Ghosh, S. (2002) *Mol. Cell* **9,** 625–636
14. Zhong, H., SuYang, H., Erdjument-Bromage, H., Tempst, P., and Ghosh, S. (1997) *Cell* **89,** 413–424
15. Vermeulen, L., De Wilde, G., Van Damme, P., Vanden Berghe, W., and Haegeman, G. (2003) *EMBO J.* **22,** 1313–1324
16. Duran, A., Diaz-Meco, M. T., and Moscat, J. (2003) *EMBO J.* **22,** 3910–3918
17. Chen, L., Fischle, W., Verdin, E., and Greene, W. C. (2001) *Science* **293,** 1653–1657
18. Chen, L. F., Mu, Y., and Greene, W. C. (2002) *EMBO J.* **21,** 6539–6548
19. Chen, L. F., and Greene, W. C. (2003) *J. Mol. Med.* **81,** 549–557
20. Kiernan, R., Bres, V., Ng, R. W., Coudart, M. P., El Messaoudi, S., Sardet, C., Jin, D. Y., Emiliani, S., and Benkirane, M. (2003) *J. Biol. Chem.* **278,** 2758–2766
21. Benezra, M., Chevallier, N., Morrison, D. J., MacLachlan, T. K., El-Deiry, W. S., and Licht, J. D. (2003) *J. Biol. Chem.* **278,** 26333–26341
22. Hung, L. Y., Tang, C. J., and Tang, T. K. (2000) *Mol. Cell. Biol.* **20,** 7813–7825
23. Peng, B., Sutherland, K. D., Sum, E. Y., Olayioye, M., Wittlin, S., Tang, T. K., Lindeman, G. J., and Visvader, J. E. (2002) *Mol. Endocrinol.* **16,** 2019–2033
24. Watashi, K., Hijikata, M., Tagawa, A., Doi, T., Marusawa, H., and Shimotohno, K. (2003) *Mol. Cell. Biol.* **23,** 7498–7509
25. Masui, O., Ueda, Y., Tsumura, A., Koyanagi, M., Hijikata, M., and Shimotohno, K. (2002) *Int. J. Mol. Med.* **9,** 489–493
26. Soutoglou, E., Katrakili, N., and Talianidis, I. (2000) *Mol. Cell* **5,** 745–751
27. Yoshida, E., Aratani, S., Itou, H., Miyagishi, M., Takiguchi, M., Osumu, T., Murakami, K., and Fukamizu, A. (1997) *Biochem. Biophys. Res. Commun.* **241,** 664–669
28. Marusawa, H., Hijikata, M., Chiba, T., and Shimotohno, K. (1999) *J. Virol.* **73,** 4713–4720
29. Watashi, K., Hijikata, M., Marusawa, H., Doi, T., and Shimotohno, K. (2001) *Virology* **286,** 391–402
30. Bannister, A. J., and Kouzarides, T. (1996) *Nature* **384,** 641–643
31. Ogryzko, V. V., Schiltz, R. L., Russanova, V., Howard, B. H., and Nakatani, Y. (1996) *Cell* **87,** 953–959
32. Yang, X. J., Ogryzko, V. V., Nishikawa, J., Howard, B. H., and Nakatani, Y. (1996) *Nature* **382,** 319–324
33. Spencer, T. E., Jenster, G., Burcin, M. M., Allis, C. D., Zhou, J., Mizzen, C. A., McKenna, N. J., Onate, S. A., Tsai, S. Y., Tsai, M. J., and O'Malley, B. W. (1997) *Nature* **389,** 194–198
34. Chen, H., Lin, R. J., Schiltz, R. L., Chakravarti, D., Nash, A., Nagy, L., Privalsky, M. L., Nakatani, Y., and Evans, R. M. (1997) *Cell* **90,** 569–580
35. Kawasaki, H., Schiltz, L., Chiu, R., Itakura, K., Taira, K., Nakatani, Y., and Yokoyama, K. K. (2000) *Nature* **405,** 195–200
36. Yang, J. P., Hori, M., Sanda, T., and Okamoto, T. (1999) *J. Biol. Chem.* **274,** 15662–15670
37. Wu, R. C., Qin, J., Hashimoto, Y., Wong, J., Xu, J., Tsai, S. Y., Tsai, M. J., and O'Malley, B. W. (2002) *Mol. Cell. Biol.* **22,** 3549–3561
38. Fukasawa, K., Choi, T., Kuriyama, R., Rulong, S., and Vande Woude, G. F. (1996) *Science* **271,** 1744–1747
39. Tarapore, P., and Fukasawa, K. (2002) *Oncogene* **21,** 6234–6240
40. Hsu, L. C., and White, R. L. (1998) *Proc. Natl. Acad. Sci. U. S. A.* **95,** 12983–12988
41. Deng, C. X. (2002) *Oncogene* **21,** 6222–6227

Available online at www.sciencedirect.com

SCIENCE DIRECT

Virology 331 (2005) 407–417

VIROLOGY

www.elsevier.com/locate/yviro

Suppression of hepatitis C virus replicon by TGF-β

Takayuki Murata, Takayuki Ohshima, Masashi Yamaji, Masahiro Hosaka, Yusuke Miyanari, Makoto Hijikata, Kunitada Shimotohno*

Department of Viral Oncology, Institute for Virus Research, Kyoto University, Sakyo-ku, Kyoto 606-8507, Japan

Received 24 July 2004; returned to author for revision 25 August 2004; accepted 20 October 2004

Abstract

Hepatitis C virus (HCV) is one of the major causative agents of liver diseases, such as liver inflammation, fibrosis, cirrhosis, and hepatocellular carcinoma. Using an efficient HCV subgenomic replicon system, we demonstrate that transforming growth factor-beta (TGF-β) suppresses viral RNA replication and protein expression from the HCV replicon. We further show that the anti-viral effect of this cytokine is associated with cellular growth arrest in a manner dependent on Smad signaling, not mitogen-activated protein kinase (MAPK) signaling. These results suggest a novel insight into the mechanisms of liver diseases caused by HCV.

Keywords: TGF-β; Hepatitis C virus; Replicon; Smad; MAPK

Introduction

Hepatitis C virus (HCV), a member of the *Flaviviridae* family, is an enveloped virus with a positive single-stranded 9.6-kb RNA genome (Murphy et al., 1995). The virus has been identified as the major causative agent of non-A, non-B hepatitis (Choo et al., 1989) that persistently infects several millions of people throughout the world. Although acute phase HCV infection is asymptomatic in most cases, the virus frequently establishes a persistent infection. This condition is associated with serious clinical diseases, including chronic hepatitis and liver fibrosis, which can lead to liver cirrhosis and eventually hepatocellular carcinoma (Goodman and Ishak, 1995).

Despite the clinical significance, molecular investigation of the virus has been hampered due to the lack of cell culture systems that efficiently support HCV replication. In 1999, the establishment of an HCV subgenomic replicon cell culture system (Lohmann et al., 1999) improved the situation. The subgenomic replicon RNA is composed of the HCV 5′-untranslated region (UTR) containing an internal ribosomal entry site (IRES), a neomycin phosphotransferase (*neo*) gene, the HCV nonstructural (NS) proteins 3 through 5B under the control of an encephalomyocarditis virus (EMCV) IRES, followed by the HCV 3′-UTR. The *neo* gene is expressed under the control of the HCV IRES, and thereby, gives the resistance to the cells in which replicon RNA exists. Instead of the *neo* gene, the luciferase gene can be used as a marker. Using the luciferase gene is beneficial in that it offers easy, speedy, and reliable detection. As the RNA replicates autonomously in cultured cells, this replicon system provides a unique tool for the analysis of the molecular mechanisms of HCV replication and the screening of anti-HCV compounds.

Transforming growth factor-beta (TGF-β) promotes the development of liver fibrosis and cirrhosis (Gressner et al., 2002); serum cytokine levels are associated with the severity of liver fibrosis in patients with chronic HCV (Nelson et al., 1997; Neuman et al., 2001; Tsushima et al., 1999). As high levels of TGF-β expression correlate with chronic hepatitis and cirrhosis (Calabrese et al., 2003; Shirai et al., 1994), cytokine serum concentrations serve as useful serologic markers for hepatitis, cirrhosis, and carcinoma (Song et al., 2002). Despite accumulating clinical observations, the direct effect of TGF-β on HCV replication remains unknown.

* Corresponding author. Fax: +81 75 751 3998.
E-mail address: kshimoto@virus.kyoto-u.ac.jp (K. Shimotohno).

0042-6822/$ - see front matter © 2004 Elsevier Inc. All rights reserved.
doi:10.1016/j.virol.2004.10.036

Molecular biological analyses have revealed that the cytokine is a multifunctional cytokine that regulates multiple biological functions, including cellular growth inhibition, extracellular matrix (ECM) formation, apoptosis, and cell differentiation (reviewed in Derynck and Zhang, 2003; Miyazono et al., 2000). Following receptor ligation, the activation of receptor-regulated Smad (R-Smad, Smad2, and Smad3) enhances complex formation with the common-mediator Smad (Co-Smad, Smad4). These complexes translocate to the nucleus, where they directly regulate the transcription of various target genes. TGF-β receptor ligation also activates members of the mitogen-activated protein kinase (MAPK) family, including p38 MAPK, c-Jun N-terminal kinase (JNK), and extracellular signal-regulated kinase (ERK).

In this study, we demonstrate that TGF-β inhibits HCV RNA replication and viral protein expression using a HCV subgenomic replicon system. The anti-viral effect of TGF-β was associated with growth arrest of cells and the activation of Smad, not MAPK, signaling. Our results provide insight into the mechanisms of liver disease pathogenesis caused by HCV.

Results

Construction of a highly efficient and sensitive replicon system

Although we had previously developed subgenomic HCV replicon cell lines (Kishine et al., 2002), we desired a highly efficient replicon system to study the molecular mechanisms of HCV replication. Among the G418-resistant subgenomic replicon cell lines, we identified a replicon cell clone (MH14) in which the viral RNA levels were higher than those in other replicon cells (Miyanari et al., 2003). The amount of replicon RNA present in MH14 cells was approximately five times greater than that present in typical MH5 replicon cells (Fig. 1B). The production of NS5A protein in MH14 cells was also greater (Fig. 1C), suggesting efficient replication of the viral RNA. Sequence analysis of replicon RNA in the MH14 cells revealed two point mutations; S2204R, the replacement of the Ser residue at position 2204 with Arg, and a silent mutation L1882L in the NS4B coding region, which did not encode an amino acid substitution. The S2204R mutation corresponded to a previously reported adaptive mutation in NS5A (Lohmann et al., 2003). At least two forms of NS5A, p56 (basally phosphorylated form), and p58 (hyper-phosphorylated form), have been reported. Residue Ser-2204 is important for hyper-phosphorylation of the protein (Tanji et al., 1995). As expected, only the basally phosphorylated p56 form was detected and hyper-phosphorylated p58 was missing in the MH14 cells, while MH5 cells, which do not carry a mutation at the sequences liable for the hyper-phosphorylation, produce both the p56 and p58 forms of NS5A (Fig. 1C).

To test permissiveness of MH14 cells for HCV replication, cells were cured of the HCV replicon RNA by prolonged treatment with IFN-α,resulting in the curedMH14 line (Figs. 1B, C). MH5 replicon cells were treated with IFN-α in parallel, for use as controls. To examine permissiveness, cured cells were transfected with replicon RNAs in which the firefly luciferase gene was inserted (Fig. 1A). We, here, used luciferase gene as a marker since it is more convenient and has the sensitivity for better quantitation. Cells were harvested at various time points after transfection and cellular luciferase activities were measured subsequently (Figs. 1D–F). Luciferase activity in transfected cells reflects the replication of the replicon RNA. Polymerase-defective RNA replicon constructs, in which the catalytic GDD motif of the NS5B polymerase was substituted to the inactive GHD motif, were used as negative controls. When cells were transfected with the prototype NN replicon RNA, luciferase activity decreased rapidly 3 to 5 days after transfection (Figs. 1D–F, NN). Use of the MH14 RNA, which is identical to the prototype NN RNA with the exception of the L1882L and S2204R mutations, resulted in higher luciferase activities (Figs. 1D–F, MH14) than those observed in cells transfected with the NN RNA. For the curedMH14 cells, luciferase activity did not decrease (Fig. 1F, MH14), but increased, peaking 3 to 5 days after transfection, suggesting highly efficient replication.

We also tested the effect of the mutations and cured cell lines on G418-resistance transduction efficiencies (not shown) and confirmed that the numbers of G418-resistant colonies exhibited a similar trend as seen for the luciferase activities described above.

These results suggest that the curedMH14 cells were highly permissive for replication of RNA containing the adaptive mutations.

Furthermore, when curedMH14 cells were transfected with the highest efficiency replicon RNA, high luciferase activity persisted for greater than 1 month (data not shown) in the absence of selection.

Suppression of HCV replicon with luciferase by TGF-β

As we have constructed a highly efficient and sensitive replicon system using a luciferase reporter and curedMH14 cells, we used this system to screen anti-HCV compounds. Treatment for 3 days with IFN-α, IL-1β, or cyclosporin A reduced the observed luciferase activities to 3.8%, 9.5%, or 3.4% of control levels, respectively (Fig. 2A). As all three treatments have been reported to repress HCV replicon (Blight et al., 2000; Watashi et al., 2003; Zhu and Liu, 2003), the system is an effective method to screen for potential anti-HCV drugs. We also observed the suppressive effect of TGF-β on luciferase activity (Fig. 2A). While treatment with 2 ng/ml TGF-β (Fig. 2B, open circle) for 36 h had little effect on luciferase activity, enzymatic activity decreased to 11%, 12%, 10% that of the mock-treated cells (black circle) at 48, 60, and 72 h, respectively. To examine

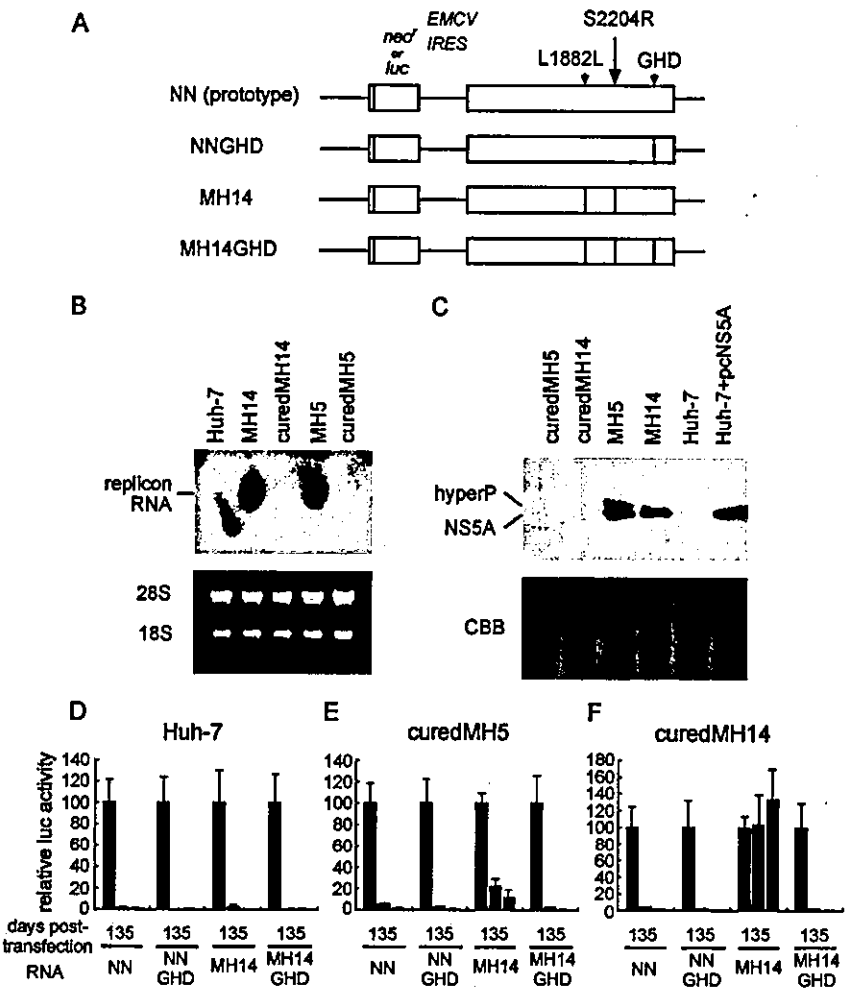

Fig. 1. Constructions and cells used in this study. (A) Schematic representation of the subgenomic replicon RNA constructs. The prototype NN RNA was used for transfection to obtain subgenomic replicon cell lines, including MH5 and MH14. NNGHD denotes polymerase-defective mutant, in which the catalytic GDD motif of the NS5B polymerase was substituted to the inactive GHD motif, and was used as a negative control. MH14 RNA carries two mutations, which were found in the replicon RNA in MH14 subgenomic replicon cells. MH14GHD is a negative control for the MH14 RNA. The ORFs are depicted as open boxes. The locations of the mutations introduced into the viral proteins are indicated by vertical lines. (B) Northern blot analysis of total RNA extracted from replicon cells. RNA from Huh-7, MH14, curedMH14, MH5, or curedMH5 cells was electrophoresed on denaturing agarose gels, blotted, and probed with an HCV RNA (upper panel). As an internal control, the ethidium bromide-staining pattern of 28S and 18S ribosomal RNA is shown (lower panel). (C) Western blot analysis of NS5A protein expressed in Huh-7, MH14, curedMH14, MH5, or curedMH5 cells (upper panel). As a control, wild-type NS5A protein was exogenously produced in Huh-7 cells from an expression plasmid (Huh-7 + pcNS5A). The position of the hyper-phosphorylated form of the protein is designated HyperP. As an internal control, the Coomassie brilliant blue (CBB) staining pattern of the same blot is shown (lower panel). (D–F) Replication of replicon RNAs with mutations in Huh-7 cells or its derivatives. Huh-7 (D), curedMH5 (E), or curedMH14 (F) cells were transfected with replicon RNA constructs containing the luciferase gene (depicted in A). Luciferase activity was measured at 1, 3, and 5 days after transfection. Each bar represents the mean and SD of three independent transfections.

the effect of TGF-β on luciferase expression and activity, the pCMV-Luc, in which the firefly luciferase gene is driven under the control of the CMV promoter, was used in Fig. 2C. While TGF-β treatment repressed the luciferase expression from replicon (Fig. 2B), we found that the cytokine enhanced the luciferase expression from the CMV promoter (Fig. 2C), provably because of the activation of transcriptional factors (Derynck and Zhang, 2003; Miyazono et al., 2000).

TGF-β is a multifunctional cytokine that exerts a range of biological activities, including cell growth inhibition (Derynck and Zhang, 2003; Miyazono et al., 2000). When exposed to TGF-β, cells generally arrest in the G(1)/S phase of the cell cycle. We, therefore, examined cell growth of curedMH14 cells (Fig. 2D). As expected, the growth of curedMH14 cells was partially inhibited by cytokine treatment (Fig. 2D, open circle). As assessed by FACS, administration of TGF-β for 2–3 days resulted in G(1)/S-arrest, while a 1-day treatment had no effect on cell cycle (Fig. 2E).

Fifty percent suppression of luciferase activity, after 3 days of treatment, was observed in the presence of

approximately 0.1 ng/ml TGF-β (Fig. 2F). Cell growth started to be suppressed at similar concentrations (Fig. 2G).

Smad-dependent suppression of HCV replicon

The cellular effects of TGF-β are mediated by both type I and type II serine/threonine kinase receptors. Receptor ligation is followed by the activation of both the canonical Smad and the MAPK signaling pathways, which include p38 MAPK, JNK, and ERK (Derynck and Zhang, 2003; Miyazono et al., 2000). To clarify the signaling pathways crucial for the suppression of HCV replication, we utilized two constitutive active receptors. One constitutively active TGF-β type-I receptor, TβR-I(T/D), evokes both Smad and

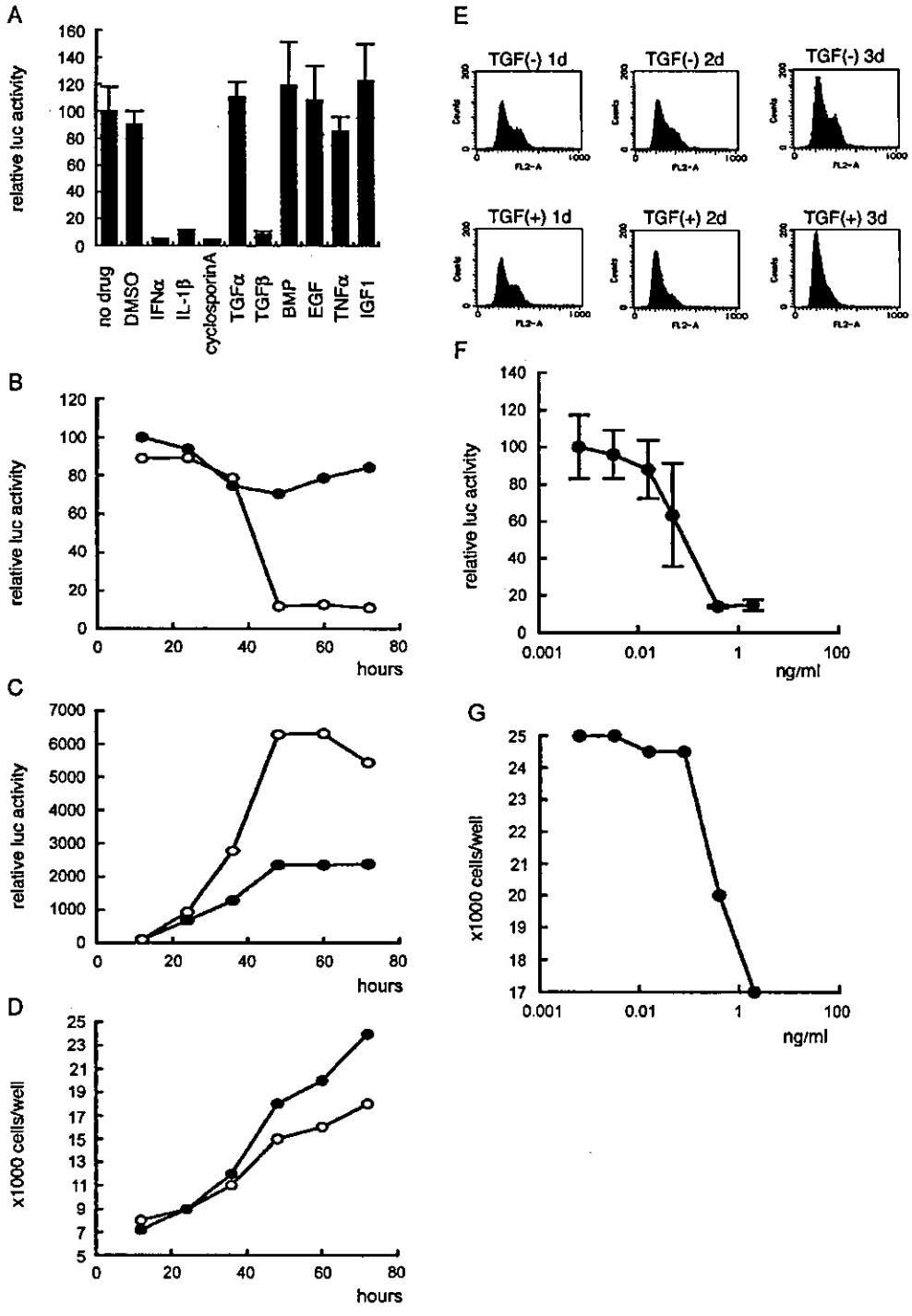

MAPK pathways, even in the absence of the TGF-β ligand (Imamura et al., 1997). The other constitutively active type-I receptor, TβR-ImL45(T/D), only activates the MAPK pathways, lacking the ability to excite Smad signaling (Yu et al., 2002). Three days after transfection of curedMH14 cells with the combination of the luciferase-replicon (LMH14) RNA and the TβR-I(T/D) expression plasmid, luciferase activity was reduced to 37% of the control levels, even in the absence of TGF-β (Fig. 3A). In contrast, co-transfection with TβR-ImL45(T/D) produces 71% of the control levels of luciferase activity, suggesting that the second constitutively active receptor had little effect on HCV replication (Fig. 3A). As summarized in Figs. 4B and C, the TβR-I(T/D) receptor likely activated transcription from promoters containing either AP-1-or Smad-responsive elements, while the TβR-ImL45(T/D) evoked transcription from the AP-1-dependent promoter alone. These data serve as evidence that the antiviral activity of TGF-β is dependent on Smad signaling.

Upon TGF-β stimulation, R-Smads specific for this cytokine, Smad2 and Smad3, are activated, forming complexes with the Co-Smad, Smad4, to activate transcription from the corresponding promoters. As co-expression of Smad2 with Smad4 or Smad3 with Smad4 mimics the effects of TGF-β stimulation (Yingling et al., 1997), we tested if such the co-expression of these molecules would also suppress HCV replicon production. Transfection of either Smad2/4 or Smad3/4 reduced the luciferase activity to 16% or 13%, respectively, even in the absence of TGF-β (Fig. 3A). Expression of an inhibitory-Smad (I-Smad), Smad7, which inhibits TGF-β mediated Smad signaling (Derynck and Zhang, 2003), only modestly reduced (81% of the control) the luciferase activity (Fig. 3A). The enhancement of transcription from AP-1-responsive (Fig. 3C), as well as TGF-β-responsive (Fig. 3B), promoters by co-transfection of either Smad2/4 or Smad3/4 was expected, as Smad4 itself has been reported to elicit transcription from AP-1 binding site-containing promoters (Liberati et al., 1999; Yingling et al., 1997).

To verify whether the Smad but not MAPK signaling is crucial for the suppression of HCV replicon by TGF-β,we used several specific MAPK inhibitors to examine if the antiviral effect of TGF-β is associated with the activation of specific MAPKs. The addition of inhibitors of ERK, p38, or JNK, U0126, SB20350, or dexamethasone, respectively, did not cancel TGF-β suppression of luciferase activity (Fig. 4A), despite effective inhibition of kinase activity by the inhibitors (Figs. 4B–D). The phosphorylation of ERK by TGF-β was not observed under these conditions (Fig. 4B), as ERK was already activated by growth factors contained within the bovine serum supplementing the culture medium.

Suppression of G418-resistant replicon by TGF-β

We then investigated the effect of TGF-β on G418-resistant replicon RNA or protein levels. MH14, G418-resistant subgenomic replicon cells, were treated with IFN-α, TGF-β, or BMP-4. BMP-4 was used here because it is a member of TGF-β superfamily cytokines and it does not induce inhibition of cell proliferation at least in Huh-7 cells. Total RNA and protein were collected at various time points. RNAs were subjected to Real-Time RT-PCR (Fig. 5A) or Northern blotting (Fig. 5B), while proteins were examined by Western blotting (Fig. 5C). Replicon RNA levels gradually decreased following treatment with 2 ng/ml TGF-β to 0.6% of the levels observed in mock-treated samples on the 7th day. This inhibition was similar to that seen following treatment with 100 IU/ml IFN-α. The NS5A protein was virtually undetectable by the 5th day after transfection (Fig. 5C). The suppressive effect of TGF-β on viral protein production was also observed by indirect immunofluorescence (not shown).

Because the replicon RNA of MH14 cells has the EMCV IRES to produce NS proteins, one could not deny the possibility that the EMCV IRES might cause the inhibition by TGF-β. Therefore, we next used full-genome replicon cell line SNC#2 (Fig. 6), which has the HCV IRES instead of the EMCV IRES, and tested if TGF-β would affect the replication. As shown in Fig. 6B, replicon RNA in SNC#2 cells treated with TGF-β decreased clearly while BMP-4 did not suppress the RNA levels.

Simultaneous suppression of viral RNA replication and protein synthesis by TGF-β

The suppression of HCV replication by TGF-β treatment was associated with the inhibition of cell growth. We examined the kinetics of the suppression of HCV replication

Fig. 2. Suppression of luciferase-replicon by TGF-β. (A) curedMH14 cells transfected with the luciferase-replicon RNA construct (LMH14), were administered with DMSO (0.1%), IFN-α (100 IU/ml), IL-1β (10 ng/ml), cyclosporin A (1 μg/ml), TGF-α (1 ng/ml), TGF-β (2 ng/ml), BMP-4 (10 ng/ml), mEGF (100 ng/ml), TNF-α (10 ng/ml), or IGF-1 (1 ng/ml). Three days later, cellular luciferase activity was measured. Bars represent the mean and SD of three independent experiments. (B) curedMH14 cells transfected with LMH14 luciferase-replicon RNA construct were mock-treated (black circle) or treated with TGF-β (2 ng/ml, white circle). At the indicated times, cells were harvested for determination of luciferase activity. The activity was normalized to cell number. (C) In parallel with the experiments in Fig. 3B, cells transfected with pCMV-Luc were mock-treated (black circle) or treated with TGF-β (2 ng/ml, white circle). At the indicated times, cells were harvested for determination of luciferase activity. The activity was normalized to cell number. (D) In parallel with the experiments in Fig. 3B, cells were mock-treated (black circle) or treated with TGF-β (2 ng/ml, white circle). Cell numbers were counted at the indicated time points. (E) Flow cytometric analysis of cell cycle progressing in curedMH14 cells transfected with the S2204R luciferase-replicon RNA construct. Cells were incubated in the presence or absence of TGF-β (2 ng/ml) for 1, 2, or 3 days. The DNA content of these cells was analyzed as described in Materials and methods. Dose-dependence of luciferase-replicon (F) and cell growth inhibition (G). curedMH14 cells transfected with the LMH14 luciferase-replicon RNA construct were treated with varying concentrations of TGF-β for 3 days. Luciferase activity (F) and cell number (G) were subsequently determined. The luciferase activity was normalized to cell number and shown with the SD value of three experiments in F.

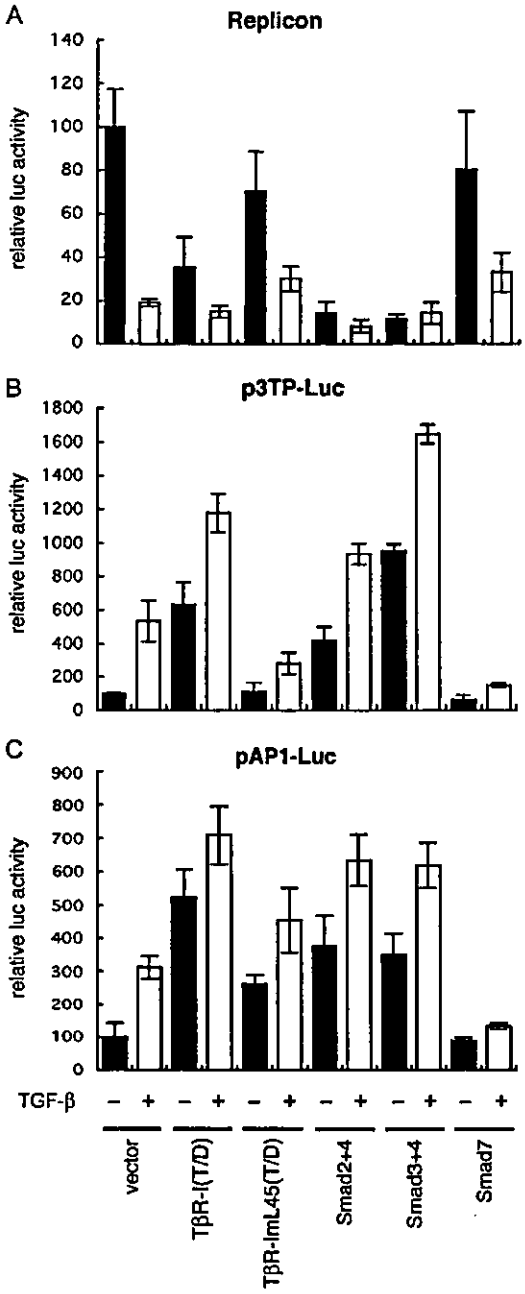

Fig. 3. Expression of TGF-β signaling-related proteins affected HCV replicon. curedMH14 cells were transfected with the expression plasmid designated below panel C together with (A) the luciferase-replicon construct with the mutations (LMH14), (B) p3TP-Luc, to monitor Smad-dependent transcription, or (C) pAP1-Luc, used to monitor AP-1-dependent transcription. Four hours after transfection, TGF-β (2 ng/ml) was added. Cells were incubated with or without the cytokine for 3 days (A) or 12 h (B, C) and then cellular luciferase activity was measured. The luciferase activity in A was normalized to cell number and then, the mean and SD value of three transfections are shown.

by examining viral RNA and protein synthesis rates at various times after the inoculation of replicon cells with the cytokine (Fig. 7). Aphidicolin and IFN-α were used as controls. The inhibition of viral protein synthesis by 100 IU/ml IFN-α began 12 h after treatment, while viral RNA synthesis was not affected until 24 h after cytokine addition. These results suggest that IFN-α first represses protein synthesis, thereby blocking RNA replication. In contrast, both aphidicolin and TGF-β inhibited protein synthesis and RNA replication concurrently, by 48 h after treatment. As both aphidicolin and TGF-β have growth inhibitory effects on cells, it is likely that both prevent HCV replicon in similar manners.

Anti-HCV activity of TGF-β was not mediated by IFN-induced signaling pathway

Although the antiviral activity of TGF-β was dependent on Smad signaling, the possibility remains that TGF-β may exert an antiviral activity via the same mechanisms as IFN-α and -γ. The binding of IFN-α or -γ to cellular receptors activates the JAK tyrosine kinase, which in turn phosphorylates effector Stat proteins. These proteins stimulate transcription from promoters with the specific sequences, ISRE or GAS, respectively. We prepared reporter plasmids that produce firefly luciferase following IFN-α or -γ stimulation by placing the gene under the control of a promoter containing either ISRE or GAS sequence. While 100 IU/ml IFN-α stimulation enhanced transcription from the ISRE-promoter 3.5-fold, enhancement of promoter activity was not observed following TGF-β treatment (Fig. 8A). The addition of 1000 IU/ml IFN-γ activated the GAS-dependent promoter by 5.8-fold, while TGF-β had little effect (Fig. 8B). The results suggest that TGF-β exerts its antiviral activity in a manner independent of IFN signaling.

Discussion

First, we have developed an efficient HCV subgenomic replicon system in this study. When maintained in cells, HCV replicon RNA often acquires cell culture-adaptive mutations. We found that the replicon RNA in MH14 cells carries two mutations, L1882L and S2204R. Among them, the S2204R, but not the L1882L, mutation was necessary and sufficient for the high efficiency (not shown). Although the mechanism by which the adaptive mutation produce high replication efficiency is not known, the interaction of the NS5A protein with a co-factor, such as hVAP-A (Gao et al., 2004; Tu et al., 1999), might explain the phenomenon.

As cytokines can play major roles in pathogenetic process during the courses of viral diseases, the relationships between viruses and cytokines, such as TGF-β, are of great importance. In this study, we found that TGF-β inhibits viral RNA replication and protein expression in the HCV replicon system.

The mechanism by which IFN-α suppresses HCV replicon is not well understood. Here, we showed that

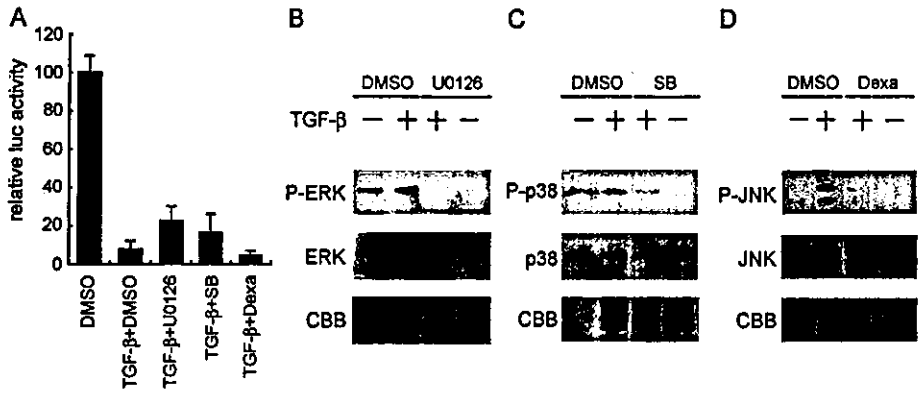

Fig. 4. Effect of MAPKs on the HCV replicon. (A) curedMH14 cells transfected with the luciferase-replicon construct (LMH14) were treated with DMSO, TGF-β (2 ng/ml) plus DMSO, or TGF-β (2 ng/ml) with either U0126 (3 μM), SB203580 (30 μM), or dexamethasone (1 μM). Inhibitors were added 1 h prior to the addition of TGF-β . After a 3-day treatment, cellular luciferase activity was measured. The mean and SD of three independent transfections are depicted after normalization to cell number. (B–D) The effect of inhibitors on the phosphorylation of ERK (B), p38MAPK (C), and JNK (D). Western blotting examined the phosphorylation of these molecules in cells treated with or without the designated reagents. The upper panels depict phosphorylated MAPKs, while the middle panels display the total amount of the MAPKs. CBB staining pattern of the same blot is used as a loading control (lower panel).

IFN-α repressed protein synthesis first, then suppressed RNA replication of the HCV replicon (Fig. 7). These data seem to support the previous report (Guo et al., 2004) and may aid our understanding of the suppression mechanism by IFN-α. IFN-α might suppress HCV translation trough the La (Shimazaki et al., 2002)-, ISG56 (Sumpter et al., 2004) or PKR (Wang et al., 2003)-dependent manner.

In contrast, either aphidicolin or TGF-β simultaneously inhibited both protein synthesis. and RNA replication from the replicon de novo (Fig. 7). While the mechanism of simultaneous suppression by aphidicolin or TGF-β remains unknown, both reagents arrest cell cycle progression at G(1)/S, suggesting a common target in the repression of HCV replicon expression. Recently, Scholle et al. (2004) reported that the replication of the HCV replicon RNA depends on host cell growth. Our results clearly correspond with that report, in which viral RNA levels remained unchanged during a 24-h period of cell cycle arrest followed by drops by 48 h.

It has been demonstrated that cell cycle arrest by TGF-β is mainly caused in the Smad pathway-dependent manner and the MAPK signaling serves as an accessory modifier of the arrest (Ten Dijke et al., 2002). Therefore, our result is convincing in that Smad, but not the MAPK pathway, played an essential role in the suppression of HCV replication.

Broadly speaking, serological investigations of HCV in chronically infected patients imply an inverse relationship between viral RNA load and TGF-β levels. Increased TGF-β expression significantly correlates with the degree of hepatic fibrosis (Calabrese et al., 2003; Nelson et al., 1997). A 3-year follow-up study demonstrated that TGF-β levels were elevated in patients with fibrosis that was

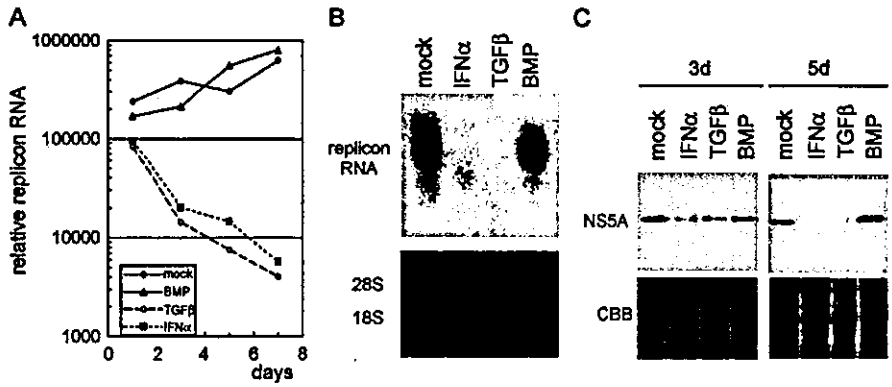

Fig. 5. Suppression of G418-resistant subgenomic replicon by TGF-β. (A) MH14, a G418-resistant subgenomic replicon cell line, was mock-treated or treated with BMP-4 (10 ng/ml), TGF-β (2 ng/ml), or IFN-α (100 IU/ml) for 1, 3, 5, or 7 days. Following the extraction of total RNA, the quantity of HCV replicon RNA was determined by real-time RT-PCR analysis. (B) Total RNA was also subjected to Northern blot analysis (upper panel). The ethidium bromide-staining pattern of ribosomal RNA is shown as an internal control (lower panel). (C) Total protein from cells prepared as above was harvested after either 3 or 5 days of cytokine treatment. Western blot analysis was performed using an antibody against NS5A. CBB staining pattern of the same blot is shown as a loading control (lower panel).

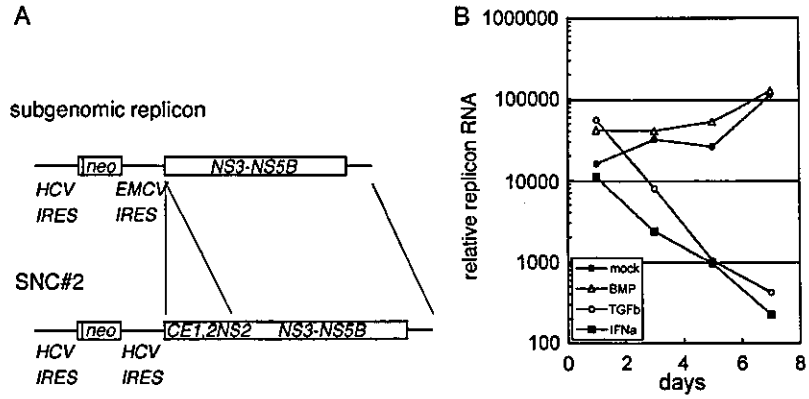

Fig. 6. Suppression of G418-resistant replicon without EMCV IRES by TGF-β. (A) Schematic representation of an RNA construct in typical subgenomic replicon cells (upper) and that in SNC#2 replicon cells (lower). RNA in SNC#2 carries the sequence for the whole HCV ORFs, driven by the HCV IRES instead of the EMCV IRES. The ORFs are depicted as open boxes. (B) SNC#2 cells were mock-treated or treated with BMP-4 (10 ng/ml), TGF-β (2 ng/ml), or IFN-α (100 IU/ml) for 1, 3, 5, or 7 days. Following the extraction of total RNA, the quantity of HCV replicon RNA was determined by real-time RT-PCR analysis.

increasing in severity (Neuman et al., 2002), which correlated with lower levels of viremia in patients than those with less progressed fibrosis (Adinolfi et al., 2001). These reports suggest that the presence of TGF-β, which may be induced by HCV core protein (Taniguchi et al., 2004), has a suppressive influence on viral RNA load. Gewaltig et al. (2002) demonstrated that polymorphisms in the TGF-β gene were associated with progression of HCV-induced liver fibrosis, suggesting again that the cytokine and the cytokine signaling have a certain influence on the virus.

The precise molecular mechanism of the anti-HCV activity of TGF-β remains to be clarified. Additional studies, including clinical studies, may reveal a novel mechanism of HCV replication regulation, potentially providing a target for novel anti-HCV therapies in the future.

Materials and methods

Cell culture, antibodies, and reagents

Huh-7, curedMH5, and curedMH14 cells were maintained in Dulbecco's modified Eagle medium (Gibco BRL) supplemented with 10% fetal bovine serum, 100 units/ml nonessential amino acids (Invitrogen), and 100 μg/ml of both penicillin and streptomycin sulfate (Invitrogen). MH5, MH14, and SNC#2 replicon cells were cultured in the above medium supplemented with 300 μg/ml G418 (Geneticin, Invitrogen). Cured cells were prepared by treating cells with 5000 IU/ml of IFN-α for 2 weeks. Absence of replicon RNA and viral proteins was checked by Northern blotting, Western blotting, and RT-PCR.

Rabbit antisera raised against p38, JNK, ERK, and phospho-ERK were purchased from Cell Signaling Tech-

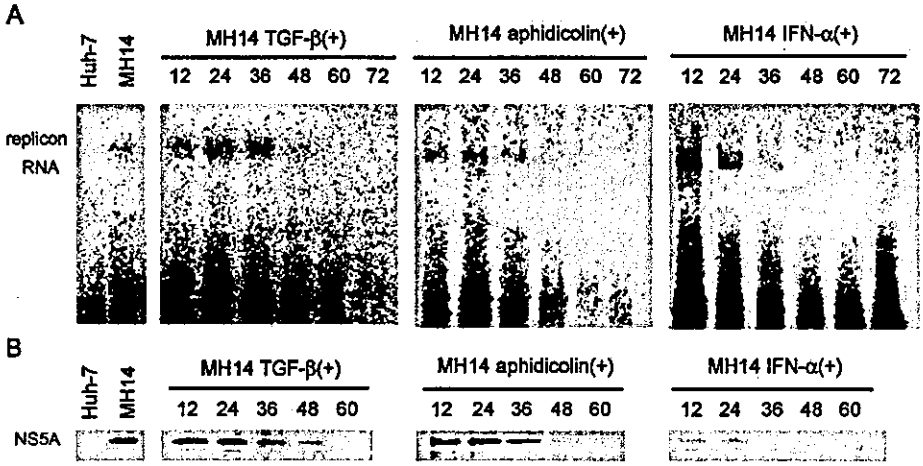

Fig. 7. Simultaneous suppression of viral RNA replication and protein synthesis by TGF-β. (A, B) MH14, a G418-resistant subgenomic replicon cell line, was mock-treated or treated with TGF-β (2 ng/ml), aphidicolin (5 μg/ml), or IFN-α (100 IU/ml) for 12, 24, 36, 48, 60, or 72 h. Cells were then subjected to semi-intact replication assay (A) or [^{35}S]-methionine metabolic labeling and immunoprecipitation using an anti-NS5A antibody (B) as described in Materials and methods.

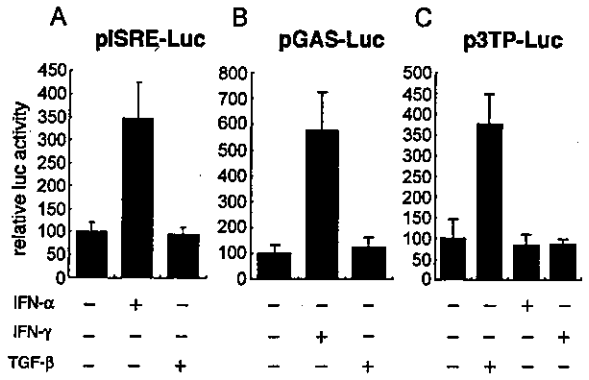

Fig. 8. TGF-β exerts an anti-HCV activity independent of the signal transduction pathway activated by IFN-α or -γ. curedMH14 cells were transfected with either pISRE-Luc (A), pGAS-Luc (B) or p3TP-Luc (C) and treated with TGF-β (2 ng/ml), IFN- (100 IU/ml), or IFN-γ (1000 IU/ml). Luciferase activities were measured 12 h after transfection. Data represent the means and SD values of relative luciferase activities in three independent experiments.

nology. Mouse antibodies specific for phospho-p38 and phospho-JNK were acquired from BD Biosciences and SIGMA, respectively. Horseradish peroxidase-conjugated goat antibodies to mouse and rabbit IgG were procured from Amersham Biosciences. TGF-β, BMP-4, and SB203580 were obtained commercially from Calbiochem. U0126 and Dexamethasone were purchased from SIGMA.

Northern and Western blot analysis

RNA was extracted from cells using Sepasol RNAI super reagent (Nacalai Tesque, Kyoto, Japan) according to the manufacturer's protocol. Northern blot analysis was performed as described (Kishine et al., 2002). The 1.5-kb *Eco*RI fragment of pNNRZ2 was used, which corresponds to the C-terminal half of the NS5A gene and the N-terminal half of the NS5B gene as a probe.

Plasmid construction

pNNRZ2 was used to prepare G418-resistant prototype NN replicon RNA (Kishine et al., 2002). To generate pMH14, L1882L and S2204R mutations in NS4B and NS5A were inserted into pNNRRZ2 by PCR-based site-directed mutagenesis. The following primers were used for mutagenesis: 5′-CTGGTCAATCTACTTCCTGCC-3′ and 5′-GGCAGGAAGTAGATTGACCAG-3′ (Bold letters in the primers denote the substituted nucleotides for L1882L). 5′-CTTCAGCTAGACAGTTGTCTGC-3′ and 5′-GCAGACAACTGTCTAGCTGAAG-3′ (same for S2204R). In addition, 5′-CACCCAAATGTACACC-AATG-3′ and 5′-CGATCCTCATGGAACCGTTC-3′, 5′-GAACGGTTCCATGAGGATCG-3′, and 5′-TGATGGG-CAGCTTGCTTTCC-3′ were used for amplification of appropriate fragments. The *neo* genes in pNNRZ2 and pMH14 were replaced with the luciferase gene from the pGL3 vector (Promega, Tokyo, Japan) to create pLNNRZ2 and pLMH14. To prepare the NS5B (RNA polymerase)-defective luciferase-replicon constructs, we inserted a GHD motif into either pLNNRZ2 or pLMH14 by replacing the corresponding sequence with pNNRZ2GHD (Kishine et al., 2002) to create pLNNRZ2GHD or pLMH14GHD, respectively. pSNC was generated to prepare G418-resistant full-genome replicon cell line, SNC#2. To prepare the plasmid, the sequence from NS3 to the end of the NS5B was cloned from I377NS3-3′ (Lohmann et al., 1999) with the S2204I adaptive mutation and other parts were from pM1LE (Kishine et al., 2002).

The coding region for NS5A in the pNNRZ2 plasmid was cloned into the *Sma*I site of pCALNL5/pBR (kindly provided by Dr. M. Kohara, Tokyo Metropolitan Institute of Medical Science). The neomycin-resistance gene was removed by *Xho*I digestion to prepare the expression vector pcNS5A.

pcDNA3 (Invitrogen)-based plasmids expressing FLAG-tagged human Smad2 or Smad4, HA-tagged constitutively active TGF-β type I receptor (TβR-I[T/D]), and p3TP-Luc have been described previously (Ohshima and Shimotohno, 2003; Imamura et al., 1997). The combined mutant type I receptor, R-ImL45(T/D), which possesses a constitutively active kinase domain, but lacks the ability to phosphorylate Smad, was generated by PCR-based mutagenesis as described (Ohshima and Shimotohno, 2003; Yu et al., 2002). The pAP1-Luc reporter plasmid was obtained commercially (PathDetect Reporter System; Stratagene, LaJolla, CA). Two additional reporter plasmids, pISRE (IFN-α-stimulated response element)-Luc and pGAS (gamma activation site)-Luc, were based on pGL3-Promoter Vector (Promega, Tokyo, Japan) that contains the SV40 basal promoter sequence without an enhancer sequence. To create pISRE-Luc, the ISRE consensus sequence (ACTTT-CAGTTTCAT) was repeated five times in tandem and inserted between the *Mlu*I and *Xho*I cloning sites of the pGL3-Promoter vector. For pGAS-Luc, three tandem repeats of the GAS sequence (TTTCCCCGAAA) were cloned into the pGL3-Promoter Vector at the *Kpn*I–*Bgl*II cleavage site.

RNA synthesis

HCV subgenomic RNA was transcribed in vitro using a MEGAscript T7 kit (Ambion) according to the manufacturer's instructions. Following DNase treatment, RNA was purified by lithium chloride precipitation.

Transfection and luciferase assay

For the luciferase assay to monitor luciferase-replicon, curedMH14 or other cells seeded on 48-well plate (5×10^3 cells/well) were transfected with 0.25 μg of the luciferase-replicon RNA using DMRIE-C reagent (Invitrogen) according to the manufacturer's instructions. Proteins in cells were